hexagon:2611.00690v1

MAXIMIZING THE FIRST POSITIVE NEUMANN EIGENVALUE OF PENTAGONS AND HEXAGONS

LÜWEI DONG AND SIRUI YANG

ABSTRACT. For $n = 5$ and $n = 6$, we prove that the regular n-gon uniquely maximizes the first positive Neumann eigenvalue of the Laplacian among all simple n-gons of prescribed area, up to congruence. Reflex and straight interior angles are allowed; polygons having them are bounded uniformly by conformal transplantation from the unit disk together with a Schwarz–Christoffel estimate that depends only on the number of strictly convex vertices. For strictly convex polygons we normalize a maximum-area vertex triangle, track the resulting unimodular pullback metric in the Rayleigh quotient, and reduce all competitors to a neighborhood of the regular n-gon where both modes of the double first eigenvalue are perturbed simultaneously. For hexagons all three maximum-triangle configurations are covered, including ties. We also exclude nonconvex quadrilaterals (completing the uniqueness of the square among simple quadrilaterals), establish the gap $|R_n|\mu_1(R_n) - |P|\mu_1(P) > 5/n^4$ for every simple nonconvex n-gon with $n \geq 4$, prove quantitative strict optimality along the full affine orbit of every regular n-gon ($n \geq 3$), and isolate the remaining $(2, 1, 1)$ chamber for heptagons. Every finite comparison is backed by exact rational or interval-arithmetic certificates.

1. Introduction and Main Results

Let $P \subset \mathbb{R}^2$ be a simple n-gon, that is, the bounded open region enclosed by a simple closed polygonal curve of n edges of positive length, with area $A = |P| > 0$. We do not assume convexity: interior angles may equal π (straight vertices) or exceed π (reflex vertices). A vertex whose interior angle is strictly less than π is called strictly convex. Since P is a bounded Lipschitz domain, the Neumann Laplacian $-\Delta$ on P has discrete spectrum

$$0 = \mu_0(P) < \mu_1(P) \leq \mu_2(P) \leq \cdots,$$

counted with multiplicity. Scaling P shows that the area-normalized eigenvalue

$$F(P) = |P|\mu_1(P), \qquad \mu_1(P) = \inf_{\substack{u \in H^1(P),\, u \neq 0 \\ \int_P u = 0}} \frac{\int_P |\nabla u|^2}{\int_P u^2},$$

is invariant under translations, orthogonal maps (including reflections), and dilations. Let R_n denote a regular n-gon.

In 2009 Laugesen asked whether R_n maximizes $F(P)$ among n-gons of fixed area [1], as a polygonal counterpart to the Szegő–Weinberger inequality for the disk. Laugesen and Siudeja settled the triangular case in [2], showing that the equilateral triangle is the unique maximizer. Endo and Osting proved the optimality of the square among convex quadrilaterals [3]. In [7], Dong and Wang resolved the pentagonal problem for all simple pentagons and obtained an upper bound for polygons having at most five strictly convex vertices. The standalone pentagon preprint also appears on Hexagon [6]. The present paper includes the pentagonal proof of [7, 6]

Date: November 19, 2026.

2020 *Mathematics Subject Classification.* Primary 35P15; Secondary 49R05, 52A10, 52A40, 65G20.

Key words and phrases. Neumann Laplacian, first positive eigenvalue, polygonal domains, Szegő–Weinberger inequality, computer-assisted proof.

with its analytic estimates and certificates in Part I, completes the hexagonal case in Part II, and develops general results for arbitrary side counts in Part III.

Theorem 1.1. *For $n \in \{5, 6\}$, every simple n-gon P of positive area satisfies*

$$|P|\mu_1(P) \le |R_n|\mu_1(R_n),$$

with equality if and only if P is similar to R_n. At fixed area, the maximizer is unique up to congruence, including reflection.

Proof of Theorem 1.1 from Parts I and II. If a simple pentagon has a reflex or straight angle, at most four of its interior angles are strictly less than π. Theorem 2.1 and Proposition 3.3 then give

$$F(P) < 10.34 < 10.35335 < F(R_5).$$

Every remaining pentagon is strictly convex, and Theorem 6.8 proves strict comparison except when P is regular. Likewise, a simple hexagon with a reflex or straight angle has at most five strictly convex corners. Theorem 7.1 handles both that class and all strictly convex hexagons, with equality only for polygons similar to R_6. Conversely, similarities preserve F, and equal area forces the scaling factor to be 1. □

Two features of the Neumann problem drive our proof and govern its extension to larger n. First, to keep convex shapes inside a compact parameter space without degeneration near flat polygons, we choose a triangle T of maximum area among the $\binom{n}{3}$ vertex triples and map it affinely onto a fixed reference triangle. If $P = LQ + b$ with $L \in \mathrm{GL}_2(\mathbb{R})$, pulling back a zero-mean trial function $v \in H^1(Q)$ changes the Euclidean gradient metric:

$$F(P) \le |Q| \frac{\int_Q \nabla v^T H \nabla v}{\int_Q v^2}, \qquad H = |\det L|\, L^{-1}L^{-T}, \qquad \det H = 1.$$

As L varies, H ranges over all 2×2 symmetric positive definite matrices of determinant 1. In Parts I and II we control H across entire affine equivalence classes by combining concavity in metric coordinates, directional covariance bounds, and conic duality for pairs of trial functions.

Second, the first positive Neumann eigenvalue of R_n is always double, because the dihedral group D_n acts irreducibly on $\mathbb{R}^2$. Under perturbation, the two modes split linearly off a kernel subspace and bend quadratically along the kernel. Our local proofs therefore retain both eigenfunctions together with their first-order variational corrections. For the pentagon, the outer affine comparison forces every competing polygon to have vertex Fourier radius $r < 231/1000$, strictly inside the annular certification radius $47/200$. For the hexagon, every closed box routed to the local argument has affine-invariant shape radius $\sigma \le 39/200$, which is covered up to $\sigma = 39/200$ by the central ball and six-annulus bounds of Lemma 7.4.

Part III turns to arbitrary side counts. In Section 8 we show that every simple nonconvex quadrilateral satisfies $|P|\mu_1(P) < 47/5 < \pi^2$ (Theorem 8.1); combined with [3], this proves that the square is the unique maximizer among all simple quadrilaterals. In Section 9 we prove the quantitative gap $F(R_n) - F(P) > 5/n^4$ for every simple nonconvex n-gon ($n \ge 4$), and in fact for every simple polygon with at most $n-1$ strictly convex vertices when $n \ge 5$ (Theorem 9.1 and Corollary 9.2). As a direct consequence, $M_n = \max_P F(P)$ is attained for every $n \ge 3$, every maximizer has n strictly convex vertices, and $M_{n+1} \ge F(R_{n+1}) > M_n + 5/(n+1)^4$ for $n \ge 4$ (Corollary 9.4).

We introduce affine-invariant Fourier coordinates for convex n-gons in Lemma 10.1. These coordinates are used in Sections 10–12, where we prove strict maximality of R_n on its affine orbit for all $n \ge 3$ (Theorem 11.1). A linear correction to the first eigenfunction sharpens that estimate (Theorem 12.1 and Corollary 12.2). This gives affine regularity for odd cyclic polygons

with equal-area step-k triangles (Proposition 12.4) and rules out stretched perturbations of R_n (Corollary 12.5).

Section 13 characterizes global optimality at fixed n by a finite polynomial covering criterion (Proposition 13.1). Section 14 shows that for $n \geq 4096$, every arc of a maximum-area triangle in a competitor has more than $n/6$ edges (Theorem 14.1), and Section 15 reduces the seven-sided case to strictly convex heptagons whose maximum-area triangles all have type $(2, 1, 1)$ (Propositions 15.1 and 15.2). Section 16 explains how to reproduce all finite comparisons from the supplementary archive.

Contents

1. Introduction and Main Results 1

Part I. Simple Pentagons 4
2. Pentagons with a Reflex or Straight Angle 4
3. The First Positive Eigenspace of the Regular Pentagon 6
4. First-Order Splitting of the Double Eigenvalue 9
5. Comparison in Vertex Fourier Coordinates 11
6. Global Comparison in Affine Coordinates 15

Part II. Simple Hexagons 21
7. The Simple Hexagon 21

Part III. Other Side Counts and Affine Comparison 30
8. Nonconvex Quadrilaterals and the Square 30
9. A Strict Comparison from the Number of Convex Corners 32
10. Affine-Invariant Fourier Coordinates for Convex n-Gons 37
11. All Affine Images of Regular Polygons 38
12. A Corrected Affine Trial and Equal-Area Vertex Triangles 39
13. A Finite Covering Criterion for Fixed Side Count 41
14. How Many Edges Can Lie on a Largest Triangle's Arcs? 42
15. The Remaining Seven-Sided Comparison 43
16. Reproducing the Finite Comparisons 45
References 46

Part I. Simple Pentagons

Throughout Part I we write $R = R_5$ and label polygon vertices in counterclockwise cyclic order.

2. Pentagons with a Reflex or Straight Angle

A reflex or straight angle lowers the number of strictly convex vertices. The bound below depends only on that count, so we state it without restricting the number of sides.

Theorem 2.1. *If a simple polygon P has at most four interior angles strictly less than π, then*

$$|P|\mu_1(P) < \frac{393329629}{38041250} < \frac{517}{50} = 10.34.$$

Rescale P to area π and pick a conformal bijection $f : \mathbb{D} \to P$ from the unit disk, rotated so that $f'(0) = \alpha > 0$. Putting

$$q(z) = \frac{f'(z)}{\alpha} = 1 + \sum_{k\geq 1} \gamma_k z^k, \qquad w_k = \frac{|\gamma_k|^2}{k+1},$$

the area formula and angular orthogonality give

$$\alpha^2 \left(1 + \sum_{k\geq 1} w_k\right) = 1.$$

Because we will select $f(0)$ to balance our Neumann trial functions, γ_1 need not vanish. We therefore state Wang's circular-mean estimate [4, Lemma 3.3] with the $k = 1$ mode kept.

Lemma 2.2. *If a simple polygon P has p strictly convex vertices, then for all $0 < \rho < 1$ and $b \geq 0$,*

$$\sum_{k\geq 1} w_k (k+1) \left(\frac{k}{2} - b\right)^2 \rho^k \geq (1+b)^2 \rho^p - b^2. \tag{2.1}$$

Proof. Discard straight vertices, leaving N vertices with interior angles $\theta_i \in (0, 2\pi) \setminus \{\pi\}$ and preimages $\xi_i \in \partial\mathbb{D}$. Set $\nu_i = (\pi - \theta_i)/(2\pi)$. Then $\nu_i > 0$ precisely at strictly convex vertices, and the turning-angle sum gives $\sum_{i=1}^N \nu_i = 1$. By the disk Schwarz–Christoffel formula, $q(z) = \prod_{i=1}^N (1 - \bar{\xi}_i z)^{-2\nu_i}$. Define

$$H(z) = \frac{z q'(z)}{2q(z)} = \sum_{i=1}^N \frac{\nu_i}{1 - \bar{\xi}_i z} - 1, \qquad L(z) = \frac{H(z) - b}{1 + b + H(z)}.$$

Between the points ξ_i on $\partial\mathbb{D}$ we have $\operatorname{Re}((1 - \bar{\xi}_i z)^{-1}) = 1/2$, so $\operatorname{Re} H = -1/2$ and $|L| = 1$. Moreover, $L(z) = 1$ occurs precisely at the simple poles ξ_i of H, where $\xi_i L'(\xi_i) = (1 + 2b)/\nu_i$. Since $b \geq 0$, as z traverses $\partial\mathbb{D}$ positively, $L(z)$ crosses 1 in the positive direction p times and in the negative direction $N - p$ times. Writing Z and B for the numbers of zeros and poles of L in $\mathbb{D}$ counted with multiplicity, the argument principle yields $Z - B = 2p - N$. Reflection across $\partial\mathbb{D}$ interchanges zeros and poles, while $\deg L = N$ because H has N simple poles; hence $Z + B = N$ and therefore $Z = p$.

Factor L as a unimodular constant times a quotient of finite Blaschke products, the numerator having degree p, and set $r = \sqrt{\rho}$. On $|z| = r$, each numerator Blaschke factor contributes at least $\log r$ to the circular mean of $\log |L|$, and denominator factors only increase that mean. Since $\log |q|$ is harmonic with value 0 at the origin, its mean is 0; by Jensen's formula, the mean

of $\log|1+b+H|$ is at least $\log(1+b)$. Applying these bounds to $q(H-b) = qL(1+b+H)$ and passing from the geometric mean to the arithmetic mean yields

$$\frac{1}{2\pi}\int_0^{2\pi} \left|q(re^{it})(H(re^{it})-b)\right|^2 dt \geq (1+b)^2 r^{2p}.$$

Circles passing through a zero or pole follow by continuity. Since $q(H-b) = \frac{1}{2}zq' - bq$ has constant term $-b$, Parseval's identity gives (2.1). □

Proof of Theorem 2.1. Take the real and imaginary parts of $\phi(re^{it}) = g(r)e^{it}$, with $\phi(0) = 0$ and

$$g(r) = r - \frac{2}{5}r^3 + \frac{9}{100}r^5 - \frac{7}{200}r^7 = \sum_{i\in\{1,3,5,7\}} c_i r^i.$$

Pull the uniform probability measure on P back to $\mathbb{D}$ by an initial conformal map $f_0 : \mathbb{D} \to P$. Averaging $\phi((z+a)/(1+\bar{a}z))$ against this pullback measure and dividing by $g(1) = 131/200$ yields a continuous map of $a \in \mathbb{D}$ which, by dominated convergence, extends to the identity on $\partial\mathbb{D}$. Its boundary degree is 1, so the average vanishes at some $a_* \in \mathbb{D}$. Precomposing f_0 with the inverse disk automorphism gives $\int_{\mathbb{D}} |f'|^2\phi = 0$, and a final rotation makes $f'(0) = \alpha > 0$ without disturbing the zero mean. The transplanted real functions are bounded on P and have finite Dirichlet energy by conformal invariance, hence lie in $H^1(P)$.

Write E for the total disk Dirichlet energy of ϕ divided by π, and M_j for its radial mass moments. Direct integration gives

$$E = 2\int_0^1 \left(g'(r)^2 + \frac{g(r)^2}{r^2}\right) r\,dr = \sum_{i,j} \frac{2(ij+1)c_i c_j}{i+j} = \frac{300481}{300000},$$

$$M_j = 2j\int_0^1 g(r)^2 r^{2j-1}\,dr = \sum_{s,t} \frac{2jc_s c_t}{2j+s+t}, \qquad M_1 = \frac{18893}{64000}.$$

The derivative g' decreases and $g'(1) = 1/200 > 0$, so g increases. The identity $M_j = \int_0^1 g(t^{1/(2j)})^2\,dt$ then shows that M_j increases with j. Adding the Rayleigh inequalities for the two real trial functions, integrating $g^2|f'|^2$ first in the angle, and inserting the area identity yields

$$F(P) \leq \pi E\,\frac{1+\sum_{k\geq 1} w_k}{M_1 + \sum_{k\geq 1} w_k M_{k+1}}. \tag{2.2}$$

Put $Q = 30433/100000$. It suffices to show that the denominator of (2.2) strictly exceeds $Q(1+\sum_{k\geq 1} w_k)$. Since $M_1 < Q$, we compensate for the constant mode by taking a positive linear combination of (2.1) at the three squared radii ρ_j in Table 1.

TABLE 1. Parameters ρ_j, b_j and weights y_j in Theorem 2.1.

j	ρ_j	b_j	$10^8 y_j$
1	9/22	1/22	12422833
2	7/10	10/21	1444049
3	15/17	11/5	95966

Set $d_j = (1+b_j)^2\rho_j^4 - b_j^2$, $a_{jk} = (k+1)(k/2-b_j)^2\rho_j^k$, and

$$\delta_0 = M_1 - Q + \sum_{j=1}^{3} y_j d_j, \qquad \delta_k = M_{k+1} - Q - \sum_{j=1}^{3} y_j a_{jk} \quad (k \geq 1).$$

Exact rational substitution gives the lower margins in Table 2.

TABLE 2. Lower margins $\lfloor 10^6 \min \delta_k \rfloor$ for $0 \le k \le 32$.

k	0	1–8	9–16	17–24	25–32
$\lfloor 10^6 \min \delta_k \rfloor$	11	11	11	11	550

For $k \ge 32$, M_{k+1} continues to increase while each a_{jk} decreases, because

$$\frac{a_{j,k+1}}{a_{jk}} \le \frac{15}{17} \cdot \frac{34}{33} \left(1 + \frac{1}{32 - 22/5}\right)^2 = \frac{9295}{9522} < 1.$$

Hence $\delta_k > 0$ for all $k \ge 0$. Since $p \le 4$, (2.1) yields $\sum_{k \ge 1} w_k a_{jk} \ge d_j$. Multiplying by y_j and summing shows that the denominator of (2.2) exceeds $Q(1 + \sum w_k)$ by at least $\delta_0 + \sum_{k \ge 1} w_k \delta_k > 0$. Thus $F(P) < \pi E/Q$; inserting $\pi < 3927/1250$ (from five terms of $\arctan(1/5)$ and two terms of $\arctan(1/239)$ in Machin's formula) gives the stated rational bound. □

3. The First Positive Eigenspace of the Regular Pentagon

For the convex comparison in Part I, let R be the regular pentagon of circumradius 1, with area $A_0 = |R|$ and first positive eigenvalue $\lambda = \mu_1(R)$. We need a lower bound on $\mu_3(R)$ to measure polynomial approximation errors in the first eigenspace, and a sharp enclosure of λ to serve as the comparison threshold.

3.1. **Crouzeix–Raviart Lower Bounds and the Spectral Gap**

We begin with a standard nonconforming finite-element lower bound, which we will reuse for R_6 in Section 7 and for R_n ($5 \le n \le 31$) in Section 11.

Lemma 3.1. *Let $\Omega \subset \mathbb{R}^2$ be a polygonal domain with a conforming triangulation $\mathcal{T}_h$ of maximum triangle diameter h. Let V_h be the Crouzeix–Raviart piecewise-linear space with matching edge averages across interior edges and free boundary edges, and let $0 = \mu_{0,h} < \mu_{1,h} \le \mu_{2,h} \le \cdots$ be its discrete Neumann eigenvalues (with broken gradient ∇_h). Then for every $k \ge 1$,*

$$\mu_k(\Omega) \ge \frac{\mu_{k,h}}{1 + (h^2/8)\mu_{k,h}}.$$

Proof. Let $K \in \mathcal{T}_h$ have diameter $h_K \le h$ and centroid g. If $w \in H^1(K)$ has mean zero on every edge of ∂K, integrating $\operatorname{div}((x-g)w) = 2w + (x-g)\cdot\nabla w$ over K gives $2\int_K w = -\int_K (x-g)\cdot\nabla w$, since $(x-g)\cdot n$ is constant along each edge. Also

$$\frac{1}{|K|}\int_K |x-g|^2 = \frac{1}{36}\sum_{e \subset \partial K} |e|^2 \le \frac{h_K^2}{12},$$

so Cauchy–Schwarz yields $|K|\bar{w}^2 \le (h_K^2/48)\|\nabla w\|^2_{L^2(K)}$, where $\bar{w} = |K|^{-1}\int_K w$. Adding the convex Poincaré inequality of Payne and Weinberger [5], $\|w - \bar{w}\|^2_{L^2(K)} \le (h_K^2/\pi^2)\|\nabla w\|^2_{L^2(K)}$, and using $1/48 + 1/\pi^2 < 1/8$ gives $\|w\|^2_{L^2(K)} \le (h_K^2/8)\|\nabla w\|^2_{L^2(K)}$.

Let $Iu \in V_h$ be the edge-average interpolant of $u \in H^1(\Omega)$ and put $e = u - Iu$. On every triangle K, $\int_K \nabla e = \int_{\partial K} e\, n = 0$, so Iu and e are orthogonal in the broken energy inner product. Pick a nonzero linear combination u of the first $k+1$ continuous Neumann modes (including constants) such that Iu is L^2-orthogonal to the first k discrete modes; this imposes

k linear equations. With $C = h/\sqrt{8}$, broken-energy orthogonality, the discrete variational principle, and Cauchy–Schwarz applied to $\|u\|_2 \le \|Iu\|_2 + \|e\|_2$ give

$$\mu_k(\Omega)\|u\|_2^2 \ge \|\nabla u\|_2^2 = \|\nabla_h(Iu)\|_2^2 + \|\nabla_h e\|_2^2 \ge \mu_{k,h}\|Iu\|_2^2 + C^{-2}\|e\|_2^2 \ge \frac{\mu_{k,h}}{1 + C^2\mu_{k,h}}\|u\|_2^2. \quad \square$$

Lemma 3.2. *The regular pentagon R satisfies*

$$A_0\mu_1(R) > \frac{3148984458240}{305231621431} > 10.31670, \qquad A_0\mu_3(R) > \frac{806191150080}{30662594077} > 26.29233.$$

Proof. Set $c = \cos(2\pi/5) = (\sqrt{5}-1)/4$ and $s = \sin(2\pi/5) = \sqrt{(5+\sqrt{5})/8}$, so $A_0 = 5s/2$. Connect the center of R to its five vertices. In each sector spanned by adjacent radial edges v, w, draw lines parallel to the three sides through $(iv + jw)/n$ $(i, j \ge 0,\ i + j \le n)$. This gives $5n^2$ congruent triangles of diameter $h = \sqrt{2 - 2c}/n$.

In each mesh triangle, label the $2\pi/5$ vertex by 0. With barycentric coordinates λ_i, the basis function opposite vertex i is $1 - 2\lambda_i$. Integrating yields local mass matrix $sI/(6n^2)$ and stiffness matrix $2G/s$, where

$$z^T G z = (1-c)\big[(z_0 - z_1)^2 + (z_0 - z_2)^2\big] + c(z_1 - z_2)^2.$$

Let H assemble G over all cells, and let W be diagonal with the number of incident triangles at each edge. Then $A_0\mu_{k,h}$ are the generalized eigenvalues of $(30n^2H/s,\, W)$. Replacing $1 - c$ and c by the integer weights 690983 and 309016 produces an assembly H_*. Because $10^6(1-c) > 690983$, $10^6 c > 309016$, and $951056 < 10^6 s < 951057$, every rational $q > 0$ satisfies

$$10^6(30n^2H - qsW) \succeq 30n^2H_* - 951057qW.$$

At $n = 16$ there are $5(3n^2 + n)/2 = 1960$ edge unknowns, and the right-hand matrix has the inertia recorded in Table 3.

TABLE 3. Inertia of $30n^2H_* - 951057qW$ for $n = 16$.

q	Negative	Zero	Positive
10347/1000	1	0	1959
2649/100	3	0	1957

The script `certify_pentagon.py` builds this mesh with `pent_mesh.py`, clears the denominator of q, eliminates at each step the active row with fewest stored entries (breaking ties by index), and rounds every Schur-complement entry outward to $2^{-192}\mathbb{Z}$. All pivot intervals exclude zero, so congruence under elimination certifies $A_0\mu_{1,h} > 10347/1000$ and $A_0\mu_{3,h} > 2649/100$. Lemma 3.1 then yields $A_0\mu_k(R) > q/(1 + h^2 q/(8A_0))$ for $k = 1, 3$. Substituting $h^2 = (2-2c)/n^2$, $A_0 = 5s/2$, and the rational bounds for c, s proves both inequalities. $\square$

It follows that $\lambda = \mu_1(R)$ has multiplicity exactly 2. Let E be the span of all positive Neumann modes on R with eigenvalue below 10. Since $A_0 < 2.378$, Lemma 3.2 gives $\mu_3(R) > 11$, so $\dim E \le 2$. For any unit vector $e \in \mathbb{R}^2$, rotational symmetry and integration on one sector give the area average of $(e \cdot x)^2$ as $(2 + c)/12$, so $e \cdot x$ has Rayleigh quotient $12/(2 + c) < 6$. Projection onto E is therefore injective on the two-dimensional space of linear coordinates, hence an isomorphism intertwining the symmetries of R. Rotation by $2\pi/5$ has no real invariant line on $\mathbb{R}^2$, so $-\Delta$ acts as a scalar on E, and reflection across any symmetry axis splits E into one even line and one odd line.

3.2. **The Reference Value**

Proposition 3.3. *For the regular pentagon R of unit circumradius,*

$$4.35446325047710240 < \mu_1(R) < 4.35446325047710250,$$

$$10.35335162333505933 < F(R) < 10.35335162333505954.$$

Proof. Place one vertex of R on the positive horizontal axis and let Ω be its upper half, with Dirichlet conditions on the horizontal cut and Neumann conditions on the other three sides. Odd reflection identifies the mixed variational space V with the odd subspace of $H^1(R)$. Since E carries the standard two-dimensional dihedral representation, it has a unique odd line, and Lemma 3.2 places every higher eigenvalue in V at or above $\Lambda = 11$.

For a nonzero conforming trial $v \in V$, set $m = \|v\|_2^2$ and $\rho = a(v,v)/m < \Lambda$, where $a(\cdot,\cdot)$ is the Dirichlet energy inner product. Suppose the energy-dual norm of $a(v,\cdot) - \rho(v,\cdot)$ is at most $\sqrt{m}\eta$. Define the compact self-adjoint operator T on (V,a) by $a(Tf,g) = (f,g)$, and write $M = 1/\mu_1(R)$, $b = 1/\Lambda$, $t = 1/\rho$. In the energy-normalized trial state, the spectral measure of T has mean t, variance at most η^2/ρ^3, and support in $[0,b] \cup \{M\}$. Taking expectations of $(M-T)(T-b) \le 0$ bounds $(M-t)(t-b)$ by η^2/ρ^3, whence

$$\frac{\rho}{1 + \eta^2\Lambda/(\rho(\Lambda-\rho))} \le \mu_1(R) \le \rho. \tag{3.1}$$

Set $c = (\sqrt{5}-1)/4$, $s = \sin(2\pi/5)$, and $a_0 = (1+\sqrt{5})/4$. In coordinates $x = X$, $y = sY$, the vertices of Ω are $(1,0)$, $(c,1)$, $(-a_0,2c)$, and $(-a_0,0)$. Dropping the common factor s from mass and energy gives gradient metric $D = \operatorname{diag}(1, s^{-2})$. Joining the average of the four vertices to each vertex and side midpoint creates eight triangles, each containing one polygon vertex. At that vertex we form twenty nested similar triangles at scales 2^{-j} $(1 \le j \le 20)$ and split each intervening trapezoid into two triangles, obtaining 328 cells. Continuous Bernstein polynomials of degrees 14 and 16 give v and a stream function w, vanishing on the Dirichlet edge and on the Neumann boundary, respectively.

On each cell K, let the orientation-preserving affine map from the reference triangle Δ have linear part B, with $J = \det B$ and $H = JB^{-1}DB^{-T}$. Hats denote pullbacks, with contravariant Piola scaling $q = B\hat{q}/J$ for fluxes. An equilibrated flux $\hat{q}$ satisfies $\operatorname{div}\hat{q} = f := -\rho J\hat{v}$ on each cell, zero normal trace on the Neumann boundary, and matching normal traces across interior edges. Integration by parts and Cauchy–Schwarz give the admissible residual bound

$$m\eta^2 = \sum_K \int_\Delta (H\nabla\hat{v} - \hat{q})^T H^{-1}(H\nabla\hat{v} - \hat{q}).$$

To build $\hat{q}$, prescribe constant outward flux densities F_e per unit reference edge parameter: zero on Neumann edges and on interior edges outside a forest in the cell adjacency graph rooted at cells touching the horizontal edge. Each cell passes its total load $\int_\Delta f$ (including descendants) out through its parent edge with opposite signs on adjacent cells, and root cells discharge the remaining load across the horizontal edge; hence $\sum_{e\subset\partial K} F_e = \int_\Delta f$ on every cell. In reference coordinates (ξ,ζ), start with $q^0 = (0, \int_0^\zeta f(\xi,t)\,dt)$ and set the tangential derivative of a scalar polynomial ψ along $\partial\Delta$ (counterclockwise) to F_e minus the existing normal flux density. By load balance this derivative integrates to zero around $\partial\Delta$; integrating from zero gives degree-16 boundary traces, which we extend into Δ by zero interior Bernstein coefficients. With $\operatorname{curl} h = (h_\zeta, -h_\xi)$, $\hat{q} = q^0 + \operatorname{curl}(\psi + \hat{w})$ has the desired divergence and normal continuity because the outward normal density of $\operatorname{curl} h$ is the tangential derivative of h.

The archived coefficients of v and w are integer multiples of 2^{-60}. Using the exact Bernstein integration formula

$$\int_\Delta B_\alpha^p B_\beta^p = \frac{(p!)^2}{(2p+2)!}\prod_{i=0}^{2}\binom{\alpha_i+\beta_i}{\alpha_i},$$

the standard-library script `check_flux.py` (with `flux_mesh.py` and `flux-witness.json`) evaluates the integrals in integer interval arithmetic on $2^{-150}\mathbb{Z}$, obtaining

$$4.3544632504771024902083 69 < \rho < 4.3544632504771024902083 70,$$
$$\eta^2 < 5.1679254 \times 10^{-17}.$$

Inserting the unrounded intervals into (3.1) and multiplying by $A_0 = 5s/2$ proves the proposition. Letting P be the spectral projection onto E, the same calculation yields $\|\nabla(I-P)v\|/\sqrt{m} < 1.1900 \times 10^{-8}$ and $\|(I-P)v\|/\sqrt{m} < 3.588 \times 10^{-9}$, because every complementary eigenvalue $\gamma \geq \Lambda$ obeys $(\gamma-\rho)^2/\gamma \geq \gamma(1-\rho/\Lambda)^2$. □

4. First-Order Splitting of the Double Eigenvalue

Set $\omega = \exp(2\pi i/5)$ and label the vertices of R by $a_j = \omega^j$ $(0 \leq j < 5)$. For counterclockwise vertices $z_0, \dots, z_4 \in \mathbb{C}$, write $c_k = \frac{1}{5}\sum_{j=0}^{4} z_j \omega^{-jk}$. Near R we have $c_1 \neq 0$, and the similarity $z \mapsto (z-c_0)/c_1$ yields the unique normalized list for this labeling,

$$z_j = a_j + \xi_2 a_j^2 + \xi_3 a_j^3 + \xi_4 a_j^4, \qquad \xi_k = \frac{c_k}{c_1}, \qquad r^2 = |\xi_2|^2 + |\xi_3|^2 + |\xi_4|^2. \tag{4.1}$$

The three complex coefficients describe all six real shape parameters. We compare Rayleigh quotients by pulling them back to R, beginning with a polynomial approximation to E and the kernel of the first variation.

4.1. Polynomial Approximation of the First Modes

In Sections 4 and 5, $\langle f \rangle = A_0^{-1}\int_R f$ denotes the area average on R, and norms use this normalization: $\|f\|_2^2 = \langle |f|^2 \rangle$, $\|\nabla f\|_2^2 = \langle |\nabla f|^2 \rangle$. Let P_0 be the L^2-projection onto E, acting separately on real and imaginary parts.

Lemma 4.1. *With $z = x + iy$ and $\rho = |z|$, define p by*

$$333p(z) = 1000z - 537z\rho^2 + 83z\rho^4 + 89\bar{z}^4 - 10\bar{z}^4\rho^2 - 17z^6.$$

Then $\|p\|_2 < 1.415$, $\|\nabla p\|_2 < 2.954$, and its projection $u = P_0 p$ satisfies

$$\|p-u\|_2 < 0.025308, \qquad \|\nabla(p-u)\|_2 < 0.084159.$$

If the real or imaginary part of p is normalized individually to unit L^2 norm, the corresponding two projection errors are below 0.017906 *and* 0.059544.

Proof. Since $p(\omega z) = \omega p(z)$, we have $\langle p \rangle = 0$. Dihedral symmetry gives $\operatorname{Re} p$ and $\operatorname{Im} p$ equal masses and equal energies, hence the same Rayleigh quotient $q = \|\nabla p\|_2^2/\|p\|_2^2$. Monomial integration gives $\langle z^a \bar{z}^d \rangle = 0$ unless $5 \mid (a-d)$, in which case barycentric expansion on $(0, 1, \omega)$ yields

$$\langle z^a \bar{z}^d \rangle = \frac{2}{(a+d+2)!}\sum_{j=0}^{a}\sum_{k=0}^{d}\binom{a}{j}\binom{d}{k}(a+d-j-k)!(j+k)!\cos\frac{2\pi(j-k)}{5}.$$

Evaluating these moments in `certify_local_radius.py` gives

$$1.99765839 < \|p\|_2^2 < 1.99765840, \qquad 8.69938239 < \|\nabla p\|_2^2 < 8.69938240, \qquad q < 4.354790.$$

For any such trial v, write $e = v - P_0 v$. Since v is orthogonal to constants and $\mu_3(R) > g := 11$, eigenfunction expansion gives

$$\|e\|_2^2 \le \|v\|_2^2 \frac{q-\lambda}{g-\lambda}, \qquad \|\nabla e\|_2^2 \le g\|v\|_2^2 \frac{q-\lambda}{g-\lambda},$$

using $\|\nabla e\|_2^2 - \lambda\|e\|_2^2 \ge (1-\lambda/g)\|\nabla e\|_2^2$ for the gradient bound. Both fractions decrease with λ; substituting $\lambda > 4.354463$ from Proposition 3.3 proves all four estimates. □

4.2. **The Kernel of the First Variation**

For a displacement ξ in (4.1), map each triangle $(0, a_j, a_{j+1})$ affinely onto the corresponding perturbed triangle while fixing the origin. Write $I + tG$ for the Jacobian on one sector along $t\xi$, and put $d = \operatorname{tr} G$. Since $\langle d\rangle$ is a rotation-invariant linear form in (ξ_2, ξ_3, ξ_4) and none of these coordinates has rotation weight zero, $\langle d\rangle = 0$. For $g, h \in E$, differentiating the area-scaled stiffness minus λ times the centered mass yields

$$B(\xi)[g,h] = \langle \nabla g^T (dI - G - G^T)\nabla h\rangle - \lambda\langle dgh\rangle. \tag{4.2}$$

Here $dI - G - G^T$ comes from $\det(I+tG)(I+tG)^{-1}(I+tG)^{-T}$, and recentering g, h contributes only at second order because $\langle g\rangle = \langle h\rangle = 0$. Regard $B(\xi)$ as a self-adjoint operator on E with the energy inner product $\langle \nabla g \cdot \nabla h\rangle$.

Lemma 4.2. *For some real $\alpha \in [-0.3, 0]$, the kernel K of $\xi \mapsto B(\xi)$ consists of all vectors with $\bar\xi_4 = \alpha\xi_3$. Its Euclidean orthogonal complement Z in the Fourier chart is a real plane, and the two eigenvalues of $B(\xi)$ are $\pm b\,\mathrm{dist}(\xi, K)$ for a constant $b > 1.7$.*

Proof. Rotation by $2\pi/5$ followed by cyclic relabeling replaces ξ_k by $\omega^{1-k}\xi_k$. Because $\operatorname{tr} B(\xi)$ is rotation invariant, it vanishes identically. On traceless symmetric forms on E, rotation acts through angle $\pm 4\pi/5$, whereas on the ξ_2-plane it acts through $-2\pi/5$. Equivariance therefore rules out any dependence on ξ_2, leaving only ξ_3 and $\bar\xi_4$ (both of weight -2).

Normalize $\operatorname{Re} p$ and $\operatorname{Im} p$ separately to unit L^2 norm, writing v_x, v_y, and set $u_i = P_0 v_i$. Their common squared norm m satisfies $0 < m \le 1$; u_x and u_y are orthogonal and have opposite parities under conjugation. For $k = 3, 4$, take the real displacement a_j^k and put $B_k = B(\xi)[u_x, u_x]$. Reflection symmetry diagonalizes B in $\{u_x, u_y\}$ along both directions, and we obtain

$$-2.075 < B_3 < -0.275, \qquad -8.502 < B_4 < -7.493.$$

Indeed, on triangle j, G maps a_j, a_{j+1} to a_j^k, a_{j+1}^k. Replacing u_x by v_x in (4.2) turns the integral into a polynomial on each sector, with error at most

$$\|L_1\|_\infty(2\sqrt{q}\,d_1 + d_1^2) + q\|d\|_\infty(2d_0 + d_0^2), \qquad L_1 = dI - G - G^T,$$

where $q = 4.354790$ bounds both trial energy and λ, and $d_0 = 0.017906$, $d_1 = 0.059544$ come from Lemma 4.1. In `certify_vertex_kernel.py`, $(s,t) \mapsto (s, (1-s)t)$ maps each triangle to $[0,1]^2$; after multiplying by the Jacobian, the integrand has degree at most 13 in each variable, so tensor Lagrange quadrature on $\{0, 1/13, \dots, 1\}$ is exact, and outward rounding to $2^{-100}\mathbb{Z}$ encloses B_3 and B_4.

Put $\alpha = -B_3/B_4 \in [-0.3, 0]$. At $(\xi_2, \xi_3, \xi_4) = (0, 1, \alpha)$ both the diagonal entry and the trace vanish, so this displacement lies in K, and its rotations span the real plane $\bar\xi_4 = \alpha\xi_3$, $\xi_2 = 0$. Since $B_4 \ne 0$ and the target rotation has no invariant line, B has two-dimensional image; thus K is the direct sum of this plane and the ξ_2-plane.

For $\zeta \in Z$, the squared operator norm $\frac{1}{2}\operatorname{tr}(B(\zeta)^2)$ is a rotation-invariant positive definite quadratic form on the plane Z, hence equals $b^2|\zeta|^2$ for some $b > 0$. In the unit ξ_4-direction, the diagonal entry on the energy-normalized vector $u_x/\sqrt{\lambda m}$ has magnitude $|B_4|/(\lambda m) >$

$7.493/4.355 > 1.72$. Since projecting this unit direction onto Z has norm at most 1, we have $b > 1.7$. □

5. Comparison in Vertex Fourier Coordinates

In the normalized chart $z_j = \omega^j + \sum_{k=2}^4 \xi_k \omega^{jk}$ with $r^2 = \sum_{k=2}^4 |\xi_k|^2$, we split the comparison at $r = 1/100$. On $r \le 1/100$ we work with the first eigenspace E of R and a first-order correction; on $1/100 \le r \le 47/200$ explicit polynomial trial functions suffice. In both regions we pull all integrals back sector by sector to R.

5.1. First-Order Splitting and Remainder Bounds

Let $I + G$ send a reference sector of R linearly to its displaced sector. Write $d = \operatorname{tr} G$, $\epsilon = \det G$, $D = 1 + d + \epsilon$, and $H = \langle D \rangle$. The real-linear map $z \mapsto Az + B\bar{z}$ taking $1, \omega$ to $1, \omega^k$ has coefficients

$$A = \frac{\omega^k - \bar{\omega}}{\omega - \bar{\omega}}, \qquad B = \frac{\omega - \omega^k}{\omega - \bar{\omega}}.$$

For $k = 2, 3, 4$, its operator norm $|A| + |B|$ equals $\phi, \phi, 1$, where $\phi = (1 + \sqrt{5})/2$. Cauchy–Schwarz therefore gives $\|G\| \le \sqrt{4 + \sqrt{5}}\, r < \frac{5}{2} r$ for $r > 0$. By Fourier orthogonality of the signed area, $\langle d \rangle = 0$. With $\lambda = \mu_1(R)$, define on zero-mean real functions on R

$$C = D(I + G)^{-1}(I + G)^{-T}, \qquad M(u, v) = \langle Duv \rangle - \frac{\langle Du \rangle \langle Dv \rangle}{H},$$

$$L(u, v) = H \langle \nabla u^T C \nabla v \rangle - \lambda M(u, v).$$

For any nonzero trial v, the centered Rayleigh quotient gives $F(P)/A_0 - \lambda \le L(v, v)/M(v, v)$. Subscripts on forms indicate homogeneous degree in ξ; set $S_1 = P_0 L_1 P_0$ and $K = \ker(\xi \mapsto S_1(\xi))$.

Lemma 5.1. *Let $\delta = \operatorname{dist}(\xi, K)$. For $0 < r \le 1/100$, there is a unit-energy trial $v \in E$ satisfying*

$$L(v, v) \le -1.7\delta + \big[k_2 + 1 + E_* + 2 + \big(a_*(r) + m_*(r)\big)r\big]r^2,$$

where $k_1 = 3.10$, $k_2 = 7.75$, $D_* = 2.36$, $E_* = 2.403$, and

$$a_*(r) = \frac{D_* k_2 + E_* k_1 + k_1 + (E_* + 1)k_2 r}{(1 - 5r/2)^2}, \qquad m_*(r) = \frac{2(1.415)E_* + (2 + E_*^2)r}{1 - r^2}. \tag{5.1}$$

Proof. On E, S_1 is the form (4.2). By Lemma 4.2 its smaller eigenvalue is $-b\delta$ with $b > 1.7$; take a corresponding unit-energy eigenvector $v \in E$. From the equation of K, $\delta = |\xi_4 - \alpha\bar{\xi}_3|/\sqrt{1 + \alpha^2}$ with $\alpha \in [-0.3, 0]$.

Write $Gz = az + b'\bar{z}$ on each sector. The moduli of the coefficients of ξ_2, ξ_3, ξ_4 are $1, \phi^{-1}, 0$ in a and $\phi^{-1}, 1, 1$ in b', so $|a| \le 1.18r$, $|b'| \le 1.55r$, $|d| \le D_* r$, and $|\epsilon| \le E_* r^2$. The Fourier area formula yields $|\langle \epsilon \rangle| \le r^2$, and averaging the two frequencies in a gives $\langle d^2 \rangle = 2(|\xi_2|^2 + |\xi_3|^2/\phi^2) \le 2r^2$.

In the expansion of C, the terms of orders 1 and 2 are $C_1 = dI - G - G^T$ and $C_2 = GG^T - \epsilon I$, with operator norms at most $2|b'| \le k_1 r$ and $2|b'|(|a| + |b'|) \le k_2 r^2$; the same quadratic bound holds for $\operatorname{adj} G \operatorname{adj} G^T - \epsilon I$. From the exact identity

$$C - I - C_1 - C_2 = -\frac{dC_2 + \epsilon C_1 + \epsilon C_2}{D},$$

together with $D \ge (1 - 5r/2)^2$ and $\|C - I\| \le (k_1 r + k_2 r^2)/(1 - 5r/2)^2$, multiplying by $H = 1 + \langle \epsilon \rangle$ bounds the quadratic term of HC by $(k_2 + 1)r^2$ and the remainder by $a_*(r)r^3$. In M, the quadratic part $\langle \epsilon uv \rangle - \langle du \rangle \langle dv \rangle$ has L^2-form norm at most $(E_* + 2)r^2$; expanding the

product of the two means and using $|\langle du\rangle| \le \sqrt{2}\, r\|u\|_2$ and $H \ge 1 - r^2$ bounds the remainder by $m_*(r)r^3$. Since $\lambda\|v\|_2^2 = 1$, summing these bounds proves the lemma. □

5.2. **A Quadratic Deficit Near the Regular Pentagon**

Theorem 5.2. *Every convex pentagon P with $r \le 1/100$ in the chart (4.1) satisfies*

$$F(R) - F(P) \ge F(R)\frac{r^2}{50}.$$

Proof. Away from K the lower branch of S_1 already decreases at order δ. When $\delta \le 8r^2$ the linear splitting can be too small, so we correct two real trials in E and sum their comparison forms, written below via a single complex function.

Take the polynomial p of Lemma 4.1 (denominator 333) and set $u = P_0 p$ componentwise; recall $\|p - u\|_2 \le d_0 := 0.025308$, $\|\nabla(p-u)\|_2 \le d_1 := 0.084159$, $\|p\|_2 < 1.415$, and $\|\nabla p\|_2 < 2.954$. Define an $\mathbb{R}$-linear complex correction w in (ξ_2, ξ_3) as follows. For each $k \in \{2, 3\}$, order all integer pairs (a, b) with $1 \le a + b \le 9$ and $a - b \equiv k,\ 2 - k \pmod 5$ by increasing $a + b$ and then by increasing a. In that order, the coefficients of $z^a \bar{z}^b$ are the following integers divided by 10^4:

$$\begin{aligned} k = 2 :\ & 14354,\ 74843,\ 65622,\ -7531,\ -181800,\ 6668,\ -163133,\\ & -16820,\ -1566,\ 206183,\ -12458,\ 177226,\ 29357,\ 2416,\ 416,\\ & 4096,\ -90246,\ 5006,\ -67660,\ -15379,\ -1413;\\ k = 3 :\ & -1580,\ 101627,\ -546,\ 58102,\ -193837,\ -22619,\ 23956,\\ & -154971,\ 2657,\ 213330,\ 27945,\ 2768,\ -33552,\ 161428,\ -5112,\\ & -94028,\ -11530,\ 1603,\ -3896,\ 17645,\ -57858,\ -435. \end{aligned}$$

Multiply monomials of frequency k by ξ_k and those of frequency $2 - k$ by $\bar{\xi}_k$, sum over $k = 2, 3$, and subtract the mean on R to obtain w. This gives $w(\omega^{1-k}\xi_k, \omega z) = \omega w(\xi_k, z)$ and reflection equivariance. Extending all forms sesquilinearly, the real number $T = L(u + w, u + w)$ is the sum of the comparison forms on the two real trials; its orders 0 and 1 vanish by the eigenfunction equation and $\operatorname{tr} S_1 = 0$.

Write A_j, M_j for the degree-j parts of HC, M, and $L_j = A_j - \lambda M_j$. For zero-mean complex functions,

$$A_1 = C_1, \qquad A_2 = C_2 + \langle\epsilon\rangle I, \qquad A_3 = -dC_2 + (\langle\epsilon\rangle - \epsilon)C_1,$$

$$M_3(f, g) = -\langle df\rangle\overline{\langle\epsilon g\rangle} - \langle\epsilon f\rangle\overline{\langle dg\rangle}.$$

For $n = 2, 3$, put $\mathcal{T}_n(v) = L_n(v, v) + 2\operatorname{Re} L_{n-1}(v, w) + L_{n-2}(w, w)$, and abbreviate $a = \xi_2$, $b = \xi_3$, $c = \bar{\xi}_4$. Because (a, b, c) have cyclic weights $(-1, -2, -2)$ mod 5, rotation and reflection invariance yield real coefficients q_i, g_i such that

$$\mathcal{T}_2(u) = q_1|a|^2 + q_2|b|^2 + q_3|c|^2 + 2q_4 \operatorname{Re}(b\bar{c}),$$

$$\mathcal{T}_3(p) = \operatorname{Re}(g_1 a^2\bar{b} + g_2 a^2\bar{c} + g_3 ab^2 + g_4 abc + g_5 ac^2).$$

Sector-moment evaluation gives

$$q_1 < -1.19, \qquad q_2 < -15.45, \qquad q_3 < 17.45, \qquad |q_4| < 1.86,$$

$$(|g_1|, |g_2|, |g_3|, |g_4|, |g_5|) < (14,\ 4.4,\ 0.4,\ 10.5,\ 3.9),$$

$$\|\nabla w\|_2^2 \le 55r^2, \qquad \|w\|_2^2 \le 4.5r^2.$$

Specifically, the average of $z^a\bar{z}^b$ on sector j of R is

$$\langle z^a\bar{z}^b\rangle_j = \frac{2}{(a+b+2)!}\sum_{k=0}^{a}\sum_{l=0}^{b}\binom{a}{k}\binom{b}{l}(k+l)!(a+b-k-l)!\,\omega^{j(a-b)+k-l}. \tag{5.2}$$

For each real shape direction, (5.2) gives the mass and gradient Gram matrices of $1, p, w_2, w_3$, where w_k is the centered correction at unit real ξ_k. Putting $G_* = (A_2 - c_gI)\nabla p + A_1\nabla w$ and $V_* = (\epsilon - c_m)p + dw - d\langle dp\rangle$ for any $c_g, c_m \in \mathbb{R}$, writing $u = p - (p-u)$ and using orthogonality bounds $|\mathcal{T}_2(u) - \mathcal{T}_2(p)|$ by

$$2\|G_*\|_2 d_1 + (\|A_2\|_\infty + 2|c_g|)d_1^2 + \lambda\big[2\|V_*\|_2 d_0 + (\|\epsilon\|_\infty + \langle d^2\rangle + 2|c_m|)d_0^2\big].$$

We pick c_g, c_m as the nearest thousandths to the midpoints of the scalar projection intervals. Evaluating on the three axes gives q_1, q_2, q_3; differencing $(0, 1, \pm 1)$ and dividing by 4 gives q_4; evaluating at $(1, \pm 1, 0)$, $(1, 0, \pm 1)$, and $(1, 1, 1)$ gives $g_1, \dots, g_5$. On the two corrected planes, $\|\nabla w\|_2^2$ is at most $23.383, 54.005$ and $\|w\|_2^2$ is at most $1.743, 4.459$, with zero cross terms by disjoint frequencies. All bounds are verified in `certify_annular_trials.py` with outward rounding to $2^{-100}\mathbb{Z}$.

Fix $R_* = 0.01$. On $\delta \le 8r^2$, the kernel formula gives $|c|/r \le 0.3|b|/r + 0.084$. Setting $y = |b|/r$ and eliminating $|a|^2 = r^2 - |b|^2 - |c|^2$ yields

$$\frac{\mathcal{T}_2(u)}{r^2} \le -1.19 - (15.45 - 1.19)y^2 + (17.45 + 1.19)(0.3y + 0.084)^2 + 3.72y(0.3y + 0.084) < -1.02.$$

On the unit sphere, $\max|x^2y| = 2/(3\sqrt{3}) < 0.385$ and $\max|xyz| = 1/(3\sqrt{3}) < 0.193$, so $|\mathcal{T}_3(p)| < 11r^3$. Put $l_3 = D_*k_2 + E_*k_1$, $p_0 = 1.415$, $p_1 = 2.954$, $w_0 = 2.122$, and $w_1 = 7.42$. Because A_3, M_3 have norms (in units of r^3) at most $l_3 + k_1$ and $2(1.415)E_*$, while A_2, M_2 have norms (in units of r^2) at most $k_2 + 1$ and $E_* + 2$, expanding $u = p - (p - u)$ gives

$$\begin{aligned}\frac{|\mathcal{T}_3(u) - \mathcal{T}_3(p)|}{r^3} &\le (l_3 + k_1)(2p_1d_1 + d_1^2) + 2(k_2 + 1)w_1d_1 \\ &\quad + \lambda\big[2(1.415)E_*(2p_0d_0 + d_0^2) + 2(E_* + 2)w_0d_0\big] < 31.\end{aligned}$$

For orders ≥ 4, write $a_3 = a_*(R_*)$, $m_3 = m_*(R_*)$ from (5.1), and $\Delta = (1 - 5R_*/2)^2$. With $C_3 = -dC_2 - \epsilon C_1$, the stiffness remainder before multiplication by H is $-(dC_3 + \epsilon C_2 + \epsilon C_3)/D$, and multiplication by $H = 1 + \langle\epsilon\rangle$ adds $\langle\epsilon\rangle(C - I - C_1)$; for the mass remainder we expand the exact product of transported means divided by H. Thus the order-≥ 4 stiffness and mass remainders have norms (in units of r^4) bounded by

$$a_4 = \frac{D_*l_3 + E_*k_2 + E_*l_3R_*}{\Delta} + k_2 + \frac{(l_3 + E_*k_2R_*)R_*}{\Delta}, \qquad m_4 = \frac{2 + E_*^2 + 2(1.415)E_*R_*}{1 - R_*^2}.$$

Applying these to (u, u), the third-order remainders to (u, w), and the second-order bounds to (w, w) yields

$$\begin{aligned}\frac{|T - \mathcal{T}_2(u) - \mathcal{T}_3(u)|}{r^4} &\le 2\lambda(a_4 + m_4) + 2(a_3p_1w_1 + \lambda m_3p_0w_0) \\ &\quad + 55(k_2 + 1 + a_3R_*) + 4.5\lambda(E_* + 2 + m_3R_*) < 3100.\end{aligned}$$

Hence $T \le -(1.02 - 42R_* - 3100R_*^2)r^2 = -0.29r^2$. Since the total centered mass is at most $(1 + 5R_*/2)^2(p_0 + w_0R_*)^2$, testing the two real components produces a relative deficit at least $r^2/50$. On $\delta \ge 8r^2$, the uncorrected lower-branch trial of Lemma 5.1 satisfies

$$L(v, v) \le -\big[1.7(8) - k_2 - 1 - E_* - 2 - (a_3 + m_3)R_*\big]r^2$$

at unit regular energy, with centered mass times λ at most $(1+5R_*/2)^2$, again giving $r^2/50$. Equality holds at $r=0$, and all endpoint inequalities are checked in rational arithmetic in the same script. □

5.3. **Polynomial Trials on the Annulus**

Theorem 5.3. *In the vertex Fourier chart $z_j=\omega^j+\sum_{k=2}^4 \xi_k\omega^{jk}$ with $r^2=\sum_{k=2}^4|\xi_k|^2$, every convex pentagon P with $1/100\le r\le 47/200$ satisfies*

$$F(P)<10.35335162333505933<F(R).$$

Together with Theorem 5.2, we obtain $F(P)<F(R)$ throughout $0<r\le 47/200$.

Proof. Set $L=4.35446325047710240$. Squaring with $A_0^2=25(5+\sqrt{5})/32$ and applying Proposition 3.3 gives

$$A_0L<10.35335162333505933<F(R).$$

The file `annulus-trials.json` specifies seven rational polynomials $f_0,\dots,f_6$ in $z,\bar z$, where each triple (a,b,n) represents $10^{-8}nz^a\bar z^b$. On R define

$$Y=f_0+\xi_2f_1+\bar\xi_2f_2+\xi_3f_3+\bar\xi_3f_4+\xi_4(f_5+\bar f_0)+\bar\xi_4f_6.$$

The seven fields have frequencies $a-b\equiv 1,2,0,3,4,4,3 \pmod 5$, with $\xi_4\bar f_0$ mixing the two directions under affine stretching. Transplanting $\operatorname{Re}Y$ and $\operatorname{Im}Y$ via the continuous sectorwise affine fan map and centering separately yields two trial functions in $H^1(P)$.

On sector j, write the real-linear fan map as $w=a_jz+b_j\bar z$ sending ω^j,ω^{j+1} to z_j,z_{j+1}, and set $D_j=|a_j|^2-|b_j|^2$, $H=\frac15\sum_j D_j$, and $\Pi=\prod_j D_j$. Since the perturbation has operator norm less than $\frac52 r<1$ on $r\le 47/200$, every D_j is positive. With Wirtinger derivatives $U=Y_z$, $V=Y_{\bar z}$, put

$$E_j=2\langle|\bar a_jU-\bar b_jV|^2+|-b_jU+a_jV|^2\rangle_j,$$

$$m=\frac15\sum_{j=0}^4 D_j\langle Y\rangle_j,\qquad M=\frac15\sum_{j=0}^4 D_j\langle|Y|^2\rangle_j,$$

$$\mathcal{P}=\frac{H^2}{5}\sum_{j=0}^4 E_j\prod_{i\ne j}D_i-L\Pi(HM-|m|^2).$$

Since the inverse map is $z=(\bar a_jw-b_j\bar w)/D_j$, E_j/D_j is the transported energy of Y per unit regular sector area, $M-|m|^2/H$ is its total centered mass per unit regular area, and H is the area ratio. Thus $\mathcal{P}<0$ implies $F(P)<A_0L$, even if one centered component vanishes identically, because strict negativity forces $HM-|m|^2>0$.

Substituting (5.2) expands $\mathcal{P}$ into a polynomial of total degree at most 16 with 7,213 nonzero monomials, all having coefficients in $\mathbb{Q}(\sqrt5)$. Its constant term lies in $(0,\ 149434352254/2^{55}]$, all linear terms vanish, and the coefficients of $|\xi_2|^2$, $|\xi_3|^2$, and $|\xi_4|^2$ lie in $(-2.732,-2.730)$, $(-17.597,-17.594)$, and $(-18.857,-18.853)$, respectively.

To remove phase dependence, bound each monomial coefficient by an upper bound on its modulus unless all three conjugate pairs have equal exponents, in which case a signed upper bound suffices. Group by the powers of $(|\xi_2|,|\xi_3|,|\xi_4|)$, enclose $\sqrt5$ to precision 2^{-100} by integer square roots, round grouped bounds upward to $2^{-55}\mathbb{Z}$, and divide by r^2. On each radial subinterval, bound r^{d-2} at the appropriate endpoint according to the signs of $d-2$ and the grouped coefficient, including $d=0$.

Cover the unit sphere of moduli $(|\xi_2|,|\xi_3|,|\xi_4|)/r$ by the three permutations of $(1,y,z)/\sqrt q$ with $q=1+y^2+z^2$ and $0\le y,z\le 1$, and multiply by $q^8>0$. Even-degree terms pick up $q^{(16-d)/2}$; every odd-degree grouped coefficient is nonnegative, so $\sqrt q\le(1+q)/2$ yields

polynomial majorants on $[0,1]^2$ of degree at most 17 in each variable. Clearing positive denominators gives exact integer Bernstein coefficients via the univariate factor $\binom{k}{i}/\binom{n}{i}$ in each variable.

Dividing $[1/100, 47/200]$ into 45 intervals of length $1/200$ produces 135 squares, of which only one requires a single midpoint bisection. On all 136 resulting squares, every Bernstein coefficient is strictly negative. The standard-library scripts `check_annulus.py` and `annulus_five_sectors.py` (using `annulus-trials.json`) carry out the expansion, sign checks, and an independent Cartesian check of the exact identities for $D_j = \det B$ and E_j in coordinates $x = X$, $y = sY_c$ ($s = \sin(2\pi/5)$); an independent FLINT script `annulus_polynomial.py` using cyclic projection obtains identical exact coefficients. □

6. Global Comparison in Affine Coordinates

Choose a triangle T of maximum area among the ten vertex triples of a convex pentagon P. Its vertices divide ∂P into three arcs, and the other two vertices lie either on one arc or on two different arcs (Figure 1). An affine map sends T to a fixed reference triangle while recording the metric distortion in a unimodular positive definite matrix.

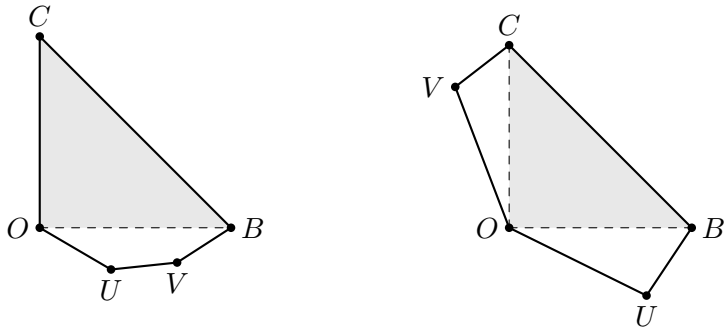


Figure 1. A maximum-area vertex triangle OBC (shaded) of a convex pentagon. Left: U, V lie on the same boundary arc from O to B. Right: U and V lie on distinct arcs, forming the two exterior triangles OUB and OCV.

6.1. **Metric Parametrization and Moment Formulas**

Up to translation, write $P = LD$, set $A = |D|$, $H = |\det L|\, L^{-1}L^{-T}$ ($\det H = 1$), and $S(f,g) = A\int_D fg - \int_D f \int_D g$. Changing variables in the Rayleigh quotient gives, for every nonconstant $f \in H^1(D)$,

$$F(P) \le \frac{A^2 \int_D \nabla f^T H \nabla f}{S(f,f)}, \qquad \det H = 1.$$

If $F(P) \ge C$, linear trials give $A^3 H \succeq CG$, where $G_{ij} = S(x_i, x_j)$. Every 2×2 symmetric positive definite matrix of determinant 1 has the form

$$H = \frac{1}{1-\rho^2}\begin{pmatrix} 1+2z+\rho^2 & 2w \\ 2w & 1-2z+\rho^2 \end{pmatrix}, \qquad \rho^2 = z^2 + w^2 < 1,$$

with $z = (H_{11} - H_{22})/(\operatorname{tr} H + 2)$, $w = 2H_{12}/(\operatorname{tr} H + 2)$, and smaller eigenvalue $(1-\rho)/(1+\rho)$. Thus $F(P) < C$ holds whenever some trial f satisfies

$$J_f = C(1-\rho^2)S(f,f) - A^2 \int_D \left[(1+2z+\rho^2)f_x^2 + 4w f_x f_y + (1-2z+\rho^2)f_y^2\right] > 0.$$

At fixed D, the quadratic part of J_f in (z,w) is $-\rho^2(CS(f,f)+A^2\int_D|\nabla f|^2)$, so J_f is concave in (z,w) and testing the four corners of a metric rectangle suffices. On a triangle with ordered vertices $0,U,V$ and $n=i+j$, barycentric integration gives

$$\int_{\triangle(0,U,V)} x^i y^j = \det(U,V)\sum_{k=0}^{i}\sum_{\ell=0}^{j}\binom{i}{k}\binom{j}{\ell}\frac{(n-k-\ell)!(k+\ell)!}{(n+2)!}\,U_x^{i-k}V_x^k U_y^{j-\ell}V_y^\ell. \tag{6.1}$$

6.2. **Both Unused Vertices on the Same Arc**

Theorem 6.1. *Let T be a triangle of maximum area among the vertex triples of a convex pentagon P. If both unused vertices lie on the same boundary arc between consecutive vertices of T, then $F(P)<103/10$. In particular, if $F(P)\ge 103/10$, every maximum-area vertex triangle has its two unused vertices on distinct arcs.*

Proof. Map T affinely to $O=(0,0)$, $B=(1,0)$, $C=(0,1)$ with counterclockwise vertex order O,U,V,B,C. Maximality of T forces every signed barycentric coordinate of U and V to lie in $[-1,1]$, so points on the exterior arc of OB take the form $(x,-y)$ with $0\le y\le x\le 1$, and O,U,V,B form a lower convex chain. Putting $U=(u,-u\alpha)$ and $v=u+(1-u)r$, concavity of the downward height y yields $u\alpha(1-r)\le -V_y\le v\alpha$. Every required shape is therefore parametrized by $(u,r,\alpha,\gamma)\in[0,1]^4$ via

$$U=(u,-u\alpha),\qquad V=(v,-d),\qquad v=u+(1-u)r,\qquad d=\alpha\big[u(1-r)+\gamma r\big].$$

Applying the area-preserving shear $(x,y)\mapsto(x,x+y)$ moves all vertices into $[0,1]^2$, with nonzero fan determinants from O equal to $u\alpha r(1-\gamma)$, d, and 1 for (U,V), (V,B), and (B,C). Each coordinate and determinant has degree at most 1 in each shape variable, so by (6.1) a monomial moment of total degree j has degree at most $j+1$ in each variable. Hence both J_f (for cubic trials) and $\det(G-A^3I/24)$ have degree at most 8 in each shape variable.

Evaluating on $\{0,1/8,\dots,1\}^4$ and inverting $W_{ij}=\binom{8}{j}(i/8)^j(1-i/8)^{8-j}$ along each axis recovers exact Bernstein coefficients. The minimum Bernstein coefficients of $(G-A^3I/24)_{11}$ and $\det(G-A^3I/24)$ are $5/576$ and $1/36864$. Thus $F(P)\ge C=103/10$ implies $H\succeq(C/24)I$ and hence $\rho\le 137/343<2/5$.

Recursive bisection of $[0,1]^4\times[-2/5,2/5]^2$, recorded in `maxtri_case_b_cover.json`, visits both closed child boxes (including their shared face) at each split. At each of its 9,447 leaves (maximum depth 41), a nonzero integer linear combination f of the nine monomials of degrees 1 through 3 has all 9^4 tensor Bernstein coefficients of J_f strictly positive at all four metric corners, so $J_f>0$ throughout the leaf by Bernstein positivity and concavity in (z,w). Initial rational matrix coefficients are rounded downward in units of 2^{-34}. Each shape bisection takes at most 8 rounds of integer averaging, so after g shape bisections the error is at most $1+8g$ units, contributing at most $(1+8g)\big(\sum_i|c_i|\big)^2$ to each quadratic form before metric weighting. All fixed-width operations are checked for overflow, two leaves are independently recomputed in arbitrary-precision integer arithmetic, and 247,927,068 strict signs are verified across the tree. □

6.3. **Boundary Exclusion for Distinct Arcs**

Theorem 6.2. *Suppose the two unused vertices of a maximum-area vertex triangle T lie on distinct boundary arcs. Map T affinely to $O=(0,0)$, $B=(1,0)$, $C=(0,1)$ with counterclockwise vertex order O,U,B,C,V. Then there exist parameters $u,v,\alpha,\beta\in[0,1]$ such that*

$$U=(u,-u\alpha),\qquad V=(-v\beta,v).$$

If $\min(u,v)\le 1/2$ or $\min(\alpha,\beta)\le 1/4$, then $F(P)<517/50=10.34$.

Proof. The barycentric argument of Theorem 6.1 gives $0 \le -U_y \le U_x \le 1$ and $0 \le -V_x \le V_y \le 1$. Apply the area-preserving change $(X, Y) = (x + y, (y - x)/2)$. Then D is the interior-disjoint union of $T = OBC$, $D_1 = OUB$, and $D_2 = OCV$, with oriented determinants $u\alpha, 1, v\beta$, and reflection in $Y = 0$ exchanges (u, α) with (v, β). Interpolation on the four-dimensional grid gives minimum Bernstein coefficients $5/576$ and $5/110592$ for $(G - A^3 I/24)_{11}$ and $\det(G - A^3 I/24)$, so $F(P) \ge C = 517/50$ forces $|z|, |w| \le 2/5$.

We use quartic trials $f(X, Y)$ with 15 integer coefficients, including the constant. On D_1 or D_2, monomial moments of total degree ≤ 8 have degree at most 9 in each ear parameter by (6.1), so ten equally spaced nodes per axis recover exact bivariate Bernstein coefficients. Put $A = \int_D 1$, $m = \int_D f$, $M = \int_D f^2$, and at a fixed metric corner set $C' = C(1 - \rho^2)$ and $E = \int_D [(1+2z+\rho^2) f_X^2 + 4w f_X f_Y + (1-2z+\rho^2) f_Y^2]$. On each box, let A_0, E_0 be the shape-midpoint values and define $L = C'M - A_0 E - E_0 A$. Enclosing each ear's contribution to L, A, E, m by its extreme bivariate Bernstein coefficients and adding the exact contribution of T yields intervals $[X_-, X_+]$; set $m_* = \max(|m_-|, |m_+|)$. Since $C'M - AE = L + A_0 E_0 - (A - A_0)(E - E_0)$ and $A_- \ge 1/2$, an explicit sufficient condition for $C'(M - m^2/A) - AE > 0$ is

$$L_- + A_0 E_0 - \max_{a \in \{A_-, A_+\},\, e \in \{E_-, E_+\}} (a - A_0)(e - E_0) > C' \frac{m_*^2}{A_-},$$

and concavity in (z, w) reduces each metric box to its four corners. By reflection symmetry, it suffices to cover $u \le 1/2$ and $\alpha \le 1/4$ (other parameters in $[0, 1]$). The trees `twoear_u_half.json` (32,691 leaves) and `twoear_alpha_quarter.json` (10,931 leaves) are checked in arbitrary-precision integer arithmetic after clearing positive denominators. □

6.4. **Covariance Bounds for Convex Competitors**

The vertex parameters above fix P only up to an affine transformation. Next we bound the anisotropy of that affine map from parallel cross-sections.

Proposition 6.3. *Let x be uniformly distributed in a convex planar polygon P, and put $X = e \cdot x$ for a unit vector e. Then*

$$\mathbb{E}[(X - \mathbb{E}X)^4] \le \frac{12}{5} \operatorname{Var}(X)^2, \qquad \mu_1(P) \operatorname{Var}(X) < \frac{35}{36}.$$

Proof. Rescale X affinely to range over $[-1, 1]$. By convexity, its density is a nonnegative piecewise-linear concave function on $[-1, 1]$, and hence a convex mixture of triangular densities of height 1 on $[-1, 1]$ with apex $T \in [-1, 1]$: subtracting the affine endpoint interpolant removes a nonnegative combination of the two endpoint triangles, and subtracting an appropriate positive multiple of the triangle peaked at each interior breakpoint cancels every downward jump in slope, leaving an affine function that vanishes at both endpoints; since each triangle integrates to 1, the mixing weights sum to 1.

Writing $m = \mathbb{E}T$, $z = \mathbb{E}T^2$, $w = \mathbb{E}T^3$, $v = \mathbb{E}T^4$, integrating each triangle gives raw moments $m/3$, $(1 + z)/6$, $(m + w)/10$, and $(1 + z + v)/15$, and expanding centered moments yields

$$15 \left(\frac{12}{5} \operatorname{Var}(X)^2 - \mathbb{E}[(X - \mathbb{E}X)^4] \right) = (z - m^2)^2 + \mathbb{E}[(1 - T^2)(T - m)^2] \ge 0.$$

Scale invariance gives the first bound. Returning to P, set $\sigma^2 = \operatorname{Var}(X)$, $Y = (X - \mathbb{E}X)/\sigma$, $k = \mathbb{E}Y^4 \le 12/5$, and test $g = Y - Y^3/24 - \mathbb{E}(Y - Y^3/24)$. Since $\operatorname{Var}(Y) = 1$ and a cubic cannot be affine on a nondegenerate interval, Cauchy–Schwarz gives $\operatorname{Var}(g) > (\mathbb{E}[Yg])^2 = (1 - k/24)^2$. The Rayleigh numerator times σ^2 is $\mathbb{E}[(1 - Y^2/8)^2] = 3/4 + k/64$. Substituting $k \le 12/5$ yields $\mu_1(P)\sigma^2 < (63/80)/(9/10)^2 = 35/36$. □

Corollary 6.4. *Let Σ be the covariance matrix of the uniform probability measure on a convex pentagon P. If $F(P) \geq F(R)$, then*

$$\sqrt{\frac{\lambda_{\max}(\Sigma)}{\lambda_{\min}(\Sigma)}} < \frac{35}{36} \cdot \frac{30 \sin(2\pi/5)}{(2+\cos(2\pi/5))\, 10.34902} < 1.161.$$

Proof. Since $|P|/\sqrt{\det \Sigma}$ is affine invariant, apply a unimodular map making Σ scalar and shift the centroid to 0. Let A_j, θ_j be the area and central angle of the j-th fan triangle, with radial side lengths r_j, r_{j+1}. Its polar moment satisfies

$$\frac{A_j}{6}(r_j^2 + r_{j+1}^2 + r_j r_{j+1} \cos\theta_j) \geq \frac{A_j^2(2+\cos\theta_j)}{3\sin\theta_j}.$$

Because $f(t) = \sin t/(2+\cos t)$ is concave on $(0,\pi)$ (its second derivative is $-2\sin t(1-\cos t)/(2+\cos t)^3 < 0$), Cauchy–Schwarz and Jensen's inequality bound the total polar moment below by $|P|^2/(3\sum_j f(\theta_j)) \geq |P|^2/(15 f(2\pi/5))$. In isotropic coordinates this equals $2|P|\sqrt{\det \Sigma}$, giving $|P|/\sqrt{\det \Sigma} \leq 30 f(2\pi/5)$. Applying Proposition 6.3 in the largest-variance direction of P and using $F(P) \geq F(R) > 10.34902$ finishes the proof. □

6.5. **Excluding Fringe Boxes by Two Simultaneous Trials**

Two trial functions produce a 2×2 matrix inequality that excludes an entire set of metrics at once, keeping the subdivision four-dimensional.

Lemma 6.5. *Let D be a planar polygon of area A, let f_1, f_2 be real polynomials, and put $B_{ij} = \int_D f_i f_j - A^{-1}\int_D f_i \int_D f_j$. For $H = \left(\begin{smallmatrix} h_1 & h_3 \\ h_3 & h_2 \end{smallmatrix}\right)$, set $\Phi(H)_{ij} = \int_D \nabla f_i^T H \nabla f_j$. Suppose a positive definite matrix H_* satisfies*

$$\det H_* > 1, \qquad CB - A\Phi(H_*) \succ 0.$$

For $c = (s,t)^T$, define $e(c) \in \mathbb{R}^3$ by $e(c)\cdot h = c^T \Phi(H) c$, where $h = (h_1, h_2, h_3)^T$. If a unimodular positive definite metric H has $\nu(H) := (h_2, h_1, -2h_3)^T$ in the convex cone generated by finitely many $e(c)$, then its first area-normalized Neumann eigenvalue is strictly less than C.

Proof. Suppose the eigenvalue were at least C. Testing all centered linear combinations of f_1, f_2 yields $A\Phi(H) \succeq CB \succ A\Phi(H_*)$, so $e(c)\cdot(h - h_*) > 0$ for all $c \neq 0$, and conic combination gives $\nu(H)\cdot(h - h_*) > 0$. Yet $\nu(H)\cdot h = 2$, while applying the arithmetic–geometric mean inequality to $H^{-1/2} H_* H^{-1/2}$ yields $\nu(H)\cdot h_* = \operatorname{tr}(H^{-1}H_*) \geq 2\sqrt{\det H_*} > 2$, a contradiction. □

Theorem 6.6. *In the distinct-arc chart of Theorem 6.2, if $\min(u,v) \leq 3/4$ or $\min(\alpha,\beta) \leq 7/16$, then $F(P) < 10.349$.*

Proof. Set $C = 10.349$, retain $(X,Y) = (x+y, (y-x)/2)$, and write $x_c = (X - \bar{X}, Y - \bar{Y})^T$ and $K = \int_D x_c x_c^T$. On an affine image TD, the pullback metric is $H = |\det T|\, T^{-1}T^{-T}$ ($\det H = 1$). Proposition 6.3 implies that $F(TD) \geq C$ requires $H \succeq M := (36C/35)K/A^2$. The polar-moment bound in Corollary 6.4 gives $A/\sqrt{\det(K/A)} < 309/25$, so $d := \det M > (36C/(35\cdot 309/25))^2 > 17/23$, while feasibility requires $d \leq 1$. Thus $M \preceq H \preceq M/d$, and after scaling by a positive p,

$$-\frac{3}{20}K \preceq pH - K \preceq \frac{3}{20}K, \qquad \text{since } \frac{1-d}{1+d} < \frac{3}{20}.$$

Writing $pH - K = K^{1/2} E K^{1/2}$ with $\|E\| \leq 3/20$ shows $|pH_{12} - K_{12}| \leq \frac{3}{20}\sqrt{K_{11}K_{22}}$, so $p\nu(H)$ is enclosed componentwise about $\nu(K)$ with radii $\frac{3}{20}K_{22}$, $\frac{3}{20}K_{11}$, and $\frac{3}{20}(K_{11}+K_{22})$.

At each trial leaf, set $Lh = (\Phi(H)_{11}, \Phi(H)_{22}, \Phi(H)_{12})^T$ and enclose $\det L$ away from zero. For the eight cyclically ordered directions

$$(1,0),\ (2,1),\ (1,1),\ (1,2),\ (0,1),\ (-1,2),\ (-1,1),\ (-2,1)$$

and $r(c) = (s^2, t^2, 2st)^T$, we have $e(c) = L^T r(c)$. Normalizing by $r_1 + r_2 = 1$ puts $(r_1 - r_2, r_3)$ in cyclic order on the unit circle, so consecutive pairs determine all eight supporting facets of their cone, and w lies in the interior precisely when $\det[r(c_i), r(c_{i+1}), w] < 0$ for every i (verified at $w = (1,1,0)^T$). Checking that $\det[e(c_i), e(c_{i+1}), p\nu(H)]$ has sign $-\operatorname{sgn}\det L$ throughout the component box ensures $L^{-T} p\nu(H)$ lies in the cone, so Lemma 6.5 applies.

Each trial leaf supplies two rational quartics and 15 integer coefficients (common denominator 2^{24}) of $H_*(s) = H_0 + \sum_{k=1}^4 H_k s_k$ on $s_k \in [-1,1]$. Checking $H_*(s) \succ 0$ and $\det H_*(s) > 1$ at all 16 corners suffices on the whole box because $\sqrt{\det X} = \inf_{Y \succ 0,\, \det Y = 1} \frac{1}{2}\operatorname{tr}(YX)$ is concave. For $R := CB - A\Phi(H_*) \succ 0$, we verify the four Gershgorin inequalities $R_{ii} \pm R_{12} > 0$. Setting $M = \int_D f_i(f_i \pm f_j)$, $m = \int_D f_i$, $m' = \int_D (f_i \pm f_j)$ $(j \neq i)$, and $Z_k = \int_D \nabla f_i^T H_k \nabla (f_i \pm f_j)$, pick rational anchors a, z_k near the box midpoints of A, Z_k with maximum deviations $\delta A, \delta Z_k$. Expanding AZ_0 and AZ_k about their anchors bounds each Gershgorin quantity below by the lower endpoint of

$$CM - aZ_0 - z_0 A + az_0 - a\sum_{k=1}^4 z_k s_k$$

minus $\delta A\, \delta Z_0 + \sum_{k=1}^4 (\delta A\, |z_k| + A_+\, \delta Z_k) + C m_* m'_* / A_-$, with bivariate Bernstein enclosures on each ear. Geometric leaves discard boxes where either multiaffine maximality inequality

$$v(1-u) + u\alpha(1+v\beta) \le 1, \qquad u(1-v) + v\beta(1+u\alpha) \le 1$$

(from $|\det(U-B, V-B)|, |\det(U-C, V-C)| \le 1$) exceeds 1 at every corner.

By Theorem 6.2 and ear-exchange symmetry, two closed boxes remain in (u, α, v, β):

$$[1/2, 3/4] \times [1/4, 1] \times [1/2, 1] \times [1/4, 1], \qquad [3/4, 1] \times [1/4, 7/16] \times [3/4, 1] \times [1/4, 1].$$

In `verify_metric_cover.py`, exact interpolation on these boxes is rounded downward to $2^{-45}\mathbb{Z}$, each midpoint subdivision takes nine rounds of integer averaging (error at most $(1+9g)2^{-45}$ after g bisections of an ear), fixed-width products are checked for overflow, and final scalar tests use arbitrary-precision integers. □

6.6. **Return to the Fourier Chart**

Proposition 6.7. *Let Q have cyclic vertices $O = (0,0)$, $U = (u, -u\alpha)$, $B = (1,0)$, $C = (0,1)$, and $V = (-v\beta, v)$, where $3/4 \le u, v \le 1$, $7/16 \le \alpha, \beta \le 1$, and*

$$v(1-u) + u\alpha(1+v\beta) \le 1, \qquad u(1-v) + v\beta(1+u\alpha) \le 1.$$

Let $P = TQ$ for an orientation-preserving invertible affine map T. If its area covariance satisfies $\sqrt{\operatorname{cond}\Sigma_P} \le 1161/1000$, then the discrete Fourier coefficients $c_k = \frac{1}{5}\sum_{j=0}^4 z_j e^{-2\pi i jk/5}$ of its physical vertices satisfy

$$c_1 \neq 0, \qquad r^2 = \frac{|c_2|^2 + |c_3|^2 + |c_4|^2}{|c_1|^2} \le \frac{11063200009}{207407376400} < \left(\frac{231}{1000}\right)^2.$$

Proof. Write $p_j \in \mathbb{R}^2$ for the chart vertices and $t_j = (\cos(2\pi j/5), \sin(2\pi j/5))^T$. The real Fourier expansion is $p_j = \bar{p} + Lt_j + Kt_{2j}$, where $L = \frac{2}{5}\sum_j p_j t_j^T$ and $K = \frac{2}{5}\sum_j p_j t_{2j}^T$. Expanding $\det L$ by pairs of columns with $\tau = (\sqrt{5}-1)/2$ gives

$$\frac{25\det L}{4\sin(2\pi/5)} = 1 + u\alpha + v\beta + \tau\big(u + v - uv(1-\alpha\beta)\big) > 0.$$

Set $H = L^{-1}K$ and $S = L^{-1}\Sigma_Q L^{-T}$. Below we verify the two chart inequalities

$$\frac{\|H\|_F}{\sqrt{2}} < \frac{7}{40}, \qquad \sqrt{\operatorname{cond} S} < \frac{11}{10}. \tag{6.2}$$

Let M be the product of the linear part of T and L, so $\Sigma_P = MSM^T$. Then $\Sigma_P^{-1/2} M S^{1/2}$ is orthogonal, whence $\operatorname{cond} M \le (1161/1000)(11/10) =: \kappa$. Writing $M(z) = Az + B'\bar{z}$ and $H(z) = ez + f\bar{z}$, positivity of $\det M$ gives $|A| > |B'|$ and singular values $|A| \pm |B'|$. Thus $c_1 = A \neq 0$, $c_4 = B'$, $|B'|/|A| \le s := (\kappa - 1)/(\kappa + 1)$, and $|e|^2 + |f|^2 = \|H\|_F^2/2$. Because the second harmonic comes from MH, we have $(c_2, c_3) = A(e, f) + B'(\bar{f}, \bar{e})$, and (6.2) implies

$$r^2 \le s^2 + (1+s)^2 \left(\frac{7}{40}\right)^2 = \frac{11063200009}{207407376400} < \left(\frac{231}{1000}\right)^2.$$

To prove (6.2), set $G_1 = 25LL^T$, $G_2 = 25KK^T$, $S_1 = \sum_j p_j p_j^T$, $h = \sum_j p_j$, and $E_1 = \sum_j (p_j p_{j+1}^T + p_{j+1} p_j^T)$ (indices modulo 5). Trigonometric identities give $G_1 = A_0 + \sqrt{5}\, A_1$ and $G_2 = A_0 - \sqrt{5}\, A_1$, where $A_0 = 5S_1 - hh^T$ and $A_1 = 2E_1 - hh^T + S_1$. Letting (X, Y) range over $(U, B), (B, C), (C, V)$ with doubled areas $d = u\alpha, 1, v\beta$, put $D = \sum d$, $m = \sum d(X + Y)$, $E = \sum d[(X+Y)(X+Y)^T + XX^T + YY^T]$, and $N = 3DE - 4mm^T = 36D^2\Sigma_Q$. With $[G, V] = \operatorname{tr}((\operatorname{adj} G)V)$, we have $\|H\|_F^2 = [G_1, G_2]/\det G_1$, and for $k = \sqrt{\operatorname{cond} S}$ we have $k + k^{-1} = [G_1, N]/\sqrt{\det G_1 \det N}$, which increases on $k \ge 1$ and equals $221/110$ at $k = 11/10$. Thus (6.2) reduces to strict positivity of

$$P_1 = 49 \det G_1 - 800[G_1, G_2], \qquad P_2 = 221^2 \det G_1 \det N - 110^2 [G_1, N]^2.$$

Both polynomials lie in $\mathbb{Q}(\sqrt{5})[u, \alpha, v, \beta]$ with individual degrees at most 4 and 12. Exact evaluation on the $(n+1)$-point uniform tensor grids ($n = 4, 12$) and axiswise Bernstein inversion yield exact Bernstein coefficients up to a positive integer factor. Bracketing $\sqrt{5}$ between $\lfloor \sqrt{5} \cdot 10^{36} \rfloor / 10^{18}$ and the next multiple of 10^{-18}, taking lower endpoints, scaling to maximum absolute value 2^{45}, and flooring gives valid lower bounds preserved under floored midpoint subdivision. Cyclic bisection in (u, α, v, β) in `verify_harmonic_bridge.py` finishes in 83 bisections (maximum depth 12) with 84 terminal boxes: 40 positive and 44 geometrically impossible by the multiaffine feasibility bounds. □

6.7. **Completion of the Convex Pentagon Case**

Theorem 6.8. *Let P be a convex pentagon of positive area. Then $F(P) \le F(R)$, with equality precisely when P is regular.*

Proof. Suppose $F(P) \ge F(R)$. By Proposition 3.3, $F(R) > 10.35335$. If P had a straight vertex it would have at most four strictly convex vertices, contradicting Theorem 2.1; thus all five vertices are strictly convex. Pick a maximum-area vertex triangle; by Theorem 6.1, its two unused vertices lie on distinct arcs. In the coordinates of Theorem 6.2, Theorem 6.6 gives $u, v > 3/4$ and $\alpha, \beta > 7/16$. Maximality of the triangle gives the two determinant inequalities in Proposition 6.7, and Corollary 6.4 gives $\sqrt{\operatorname{cond} \Sigma_P} < 1.161$. Proposition 6.7 then yields $c_1 \neq 0$ and $r < 231/1000 < 47/200$. Both $0 < r \le 1/100$ and $1/100 \le r < 231/1000$ contradict $F(P) \ge F(R)$ by Theorems 5.2 and 5.3. Hence $r = 0$, so P is regular. Conversely, similarities preserve F. □

Part II. Simple Hexagons

7. The Simple Hexagon

Theorem 7.1. *Among all simple planar polygons of positive area with at most six sides, the regular hexagon R_6 uniquely maximizes $F(P) = |P|\mu_1(P)$, up to Euclidean similarity.*

Give R_6 circumradius 1. Three benchmark constants enter the proof:

$$A_0 = |R_6| = \frac{3\sqrt{3}}{2}, \qquad L = \frac{4043}{1000}, \qquad C = \frac{105043}{10000}, \qquad A_0 L < 10.50404 < C < F(R_6).$$

Away from the regular hexagon, explicit polynomial trial functions and geometric bounds keep $F(P)$ strictly below $A_0 L$ or C. Arbitrarily close to R_6 the spectral gap tends to zero, so the local argument uses the true first eigenspace of R_6.

7.1. A Lower Bound for the Continuous Benchmark

Lemma 7.2. *For the unit-circumradius regular hexagon R_6, the full Neumann spectrum satisfies $F(R_6) > C$.*

Proof. Divide each of the six central equilateral triangles of R_6 into m^2 congruent equilateral triangles with $m = 320$, giving mesh diameter $h = 1/m$. On each cell, the Crouzeix–Raviart basis $1 - 2\lambda_i$ gives local mass matrix $sI/(6m^2)$ ($s = \sqrt{3}/2$) and stiffness matrix $2G/s$, where G is the three-node graph Laplacian with edge weights $1/2$. Matching edge means across interior edges and leaving boundary edges free gives $6m(3m+1)/2 = 922{,}560$ degrees of freedom.

At the area-scaled shift $q = 105043519/10^7$, directed integer-interval elimination in `check_regular_fan.py` yields 1 negative and 922,559 positive pivots for a lower comparison matrix. Eliminating the interior of one sector produces an exact interface matrix with diagonal blocks U, U and off-diagonal blocks V, V (by reflection symmetry, with U, V symmetric). The global cyclic interface blocks are $2(U + tV)$ for $t = \cos(2\pi k/6)$. Positive definiteness at $t = -1$ and at a rational upper bound for $t = 1/2$ rules out negative directions in every nonconstant rotation character; at $t = 1$ there is exactly one negative direction, corresponding to the constant mode. Hence $A_0\mu_{1,h} > q$.

By Lemma 3.1 with $h = 1/m$, we have $\mu_1(R_6) \geq \mu_{1,h}/(1 + h^2\mu_{1,h}/8)$. Inserting the certified shift q and rounding A_0 down gives

$$F(R_6) > \frac{37261457799945743954616320 0}{35472575611536594701681173} > C. \qquad \square$$

7.2. Polygons with at Most Five Strictly Convex Corners

Lemma 7.3. *Every simple polygon with at most five strictly convex vertices satisfies $F(P) < 1049/100$.*

Proof. Use the disk coefficients w_k of Lemma 2.2 and the balanced Rayleigh inequality (2.2) with

$$g(r) = r - \frac{5}{12}r^3 + \frac{9}{100}r^5 - \frac{1}{35}r^7, \qquad Q = \frac{355}{113} \cdot \frac{E}{1049/100}, \qquad M_j = 2j \int_0^1 g(r)^2 r^{2j-1}\, dr,$$

where $E = 2\int_0^1 ((g')^2 + g^2/r^2) r\, dr$. For the twelve integer triples (T, B, V) in Table 4, set $t = T/10^4$, $b = B/10^4$, and $v = V/10^7$.

TABLE 4. Parameters (T, B, V) for the twelve-radius combination in Lemma 7.3.

T	B	V	T	B	V	T	B	V
665	0	6073176	4303	217	478903	7820	5993	16727
2205	7	1543740	5853	1069	98816	8794	16087	1915
2425	12	391924	6435	1798	80311	8865	17545	3557
3828	120	133685	7692	5343	17144	9555	44995	401

Exact rational evaluation in `check_upper.py` yields

$$M_1 - Q + \sum v\,[(1+b)^2 t^5 - b^2] > \frac{11}{10^5},$$
$$M_{k+1} - Q - \sum v(k+1)(k/2-b)^2 t^k > \frac{70}{10^5} \qquad (1 \le k \le 256).$$

Since g increases on $[0,1]$, the moments M_j increase with j. For each triple, the ratio of consecutive cost terms at $k = 256$ is $t(258/257)(1 + 1/(256 - 2b))^2 < 1$ and decreases with k, so the second bound holds for all $k \ge 1$. Multiplying (2.1) (with $p \le 5$) by v and summing shows that the denominator of (2.2) exceeds $Q(1 + \sum w_k)$. Using $\pi < 355/113$ yields $F(P) < 1049/100$. □

7.3. **The Three Maximum-Triangle Configurations**

It remains to consider a strictly convex hexagon in counterclockwise order. Pick a triangle of maximum area among the twenty triples of vertices. Up to cycling and reversal, the numbers of unused vertices on its three open boundary arcs form one of `111`, `210`, or `300` (Figure 2). Every maximum-area constraint below is a closed inequality, so an arbitrary maximizer may be chosen in a tie. Normalizing the selected triangle uses an affine map, and we compare spectra over the entire affine class.

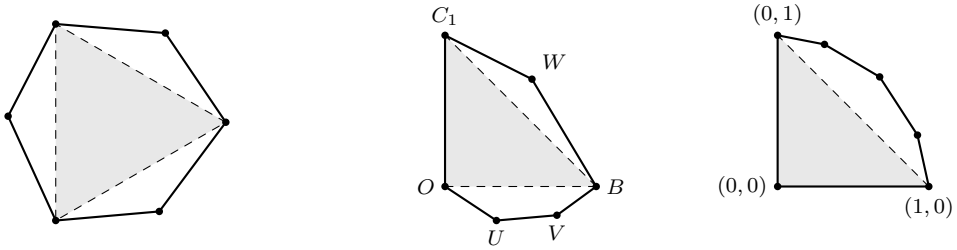


FIGURE 2. The three vertex configurations relative to a maximum-area vertex triangle (shaded) in a strictly convex hexagon: `111`, `210`, and `300`.

In configuration `300`, two sides of the maximizing triangle are consecutive polygon edges. Mapping them to $(0,0)(1,0)$ and $(0,0)(0,1)$, supporting lines and single-vertex replacements force $0 \le x, y \le 1$ on the polygon. Thus the edge $(0,0)(1,0)$ joins the parallel supporting lines $x = 0$ and $x = 1$. In any affine image, the outer normal cones at its endpoints contain opposite directions, so the two exterior turning angles sum to at least π. The adjacent-turn bound in Section 7.6 immediately gives $F(P) < C$.

In configuration `111`, use rational coordinates $X = x$, $Y = y/\sqrt{3}$, mapping the maximizing triangle to $(1,0)$, $(-1/2, 1/2)$, and $(-1/2, -1/2)$. Write the intervening vertex outside side

$i \in \{0,1,2\}$ in cyclic barycentric coordinates as $(1-p_i,\, h_i+p_i,\, -h_i)$. Convexity gives $h_i \ge 0$, and single-vertex replacement bounds every barycentric coordinate in $[-1,1]$, so

$$0 \le h_i, s_i \le 1, \qquad p_i = (1-h_i)s_i, \qquad p_i' = (1-h_i)(1-s_i), \qquad \frac{|P|}{A_0} = \frac{1+h_0+h_1+h_2}{2}$$

in this normalization. Relabeling realizes all six permutations of (h_0,h_1,h_2), while reflection reverses the tangential parameters s_i. For cyclically consecutive i,j, the two double-replacement constraints and the comparison against the other alternating triangle give (by 3×3 barycentric determinants)

$$h_i(1+h_j)+p_i(h_j+p_j) \le 1, \qquad h_j(1+h_i)+p_j'(h_i+p_i') \le 1, \qquad \sum_{i=0}^{2} h_i h_{i+1} \le \sum_{i=0}^{2} p_i p_{i+1}'.$$

At the eight corners $s_i \in \{0,1\}$, the area of the other alternating triangle (in units of the maximizing triangle) equals $1+\sum_i h_i h_{i+1}$ or a cyclic permutation of $(h_0+h_1)(1+h_2)$. Multiaffinity in s_i and monotonicity in h_i justify the interval contractions in `alternating_triangle_cover.py`.

In configuration `210`, label the boundary O,U,V,B,W,C_1 with maximizing triangle $O=(0,0)$, $B=(1,0)$, $C_1=(0,1)$. Single-vertex replacements and the supporting side OC_1 give $0 \le x \le 1$, $y \le 1$, and $x+y \ge 0$. The lower arc O,U,V,B is a lower convex graph over x, allowing a vertical terminal side VB. Set $u=x_U$, $v=x_V$, $w=x_W$, $r=(v-u)/(1-u)$, $d_U=-y_U$, $d_V=-y_V$, and $\alpha=d_U/u$. For a strictly convex hexagon we have $0<u<v\le 1$ and $w>0$, while the chord UB and the ray OU force

$$\alpha u(1-r) \le d_V \le \alpha v, \qquad t=\frac{d_V-\alpha u(1-r)}{r}, \qquad s=\alpha-t, \qquad 0 \le t \le \alpha \le 1.$$

Since $v-u(1-r)=r$ and $1-w \le y_W \le 1$, the whole `210` chart lies inside

$$\begin{aligned} &v = u+(1-u)r, && U=(u,-u(s+t)),\\ &V=(v,-su(1-r)-tv), && W=(w,1-w+w\eta),\\ &0 \le u,r,w,\eta \le 1, && s,t \ge 0, \quad s+t \le 1, \end{aligned} \tag{7.1}$$

which includes $r=1$ and $w=1$. Its doubled area is $1+us+vt+w\eta$. Applying the unimodular shear $y \mapsto y+\alpha x$ sends U,V,B,W to $(u,0)$, (v,rs), $(1,\alpha)$, and $(w,1+e)$ with $e=w(\alpha+\eta-1)$, permitting independent integration over signed triangles when the alternating-base coordinates are inconvenient.

7.4. **An Affine-Invariant Neighborhood of the Regular Hexagon**

Put $\omega=e^{\pi i/3}$, expand the vertices of a convex hexagon as $z_j=\sum_{k=0}^{5} x_k \omega^{kj}$, and translate so that $x_0=0$. For $j=0,1,2$, let $v_j=(z_j-z_{j+3})/2$. Interlacing of opposite diagonals gives $\det(v_0,v_1),\det(v_1,v_2),\det(v_0,v_2)>0$; their sum is the signed area of the centrally symmetric hexagon $(v_0,v_1,v_2,-v_0,-v_1,-v_2)$, which expands to $A_0 D$ with $D=|x_1|^2-|x_5|^2>0$. Removing the invertible real-linear map $z \mapsto x_1 z + x_5 \bar z$ leaves the canonical affine-invariant vertices

$$\begin{aligned} Q_j &= \omega^j + a\omega^{2j} + b(-1)^j + c\omega^{4j}, \qquad \sigma^2 = |a|^2+|b|^2+|c|^2,\\ (a,b,c)_k &= \frac{\bar x_1 x_k - x_5 \bar x_{6-k}}{D} \quad (k=2,3,4), \qquad \chi = \frac{|Q|}{A_0} = 1+|a|^2-|c|^2, \end{aligned} \tag{7.2}$$

where $(a,b,c)_k$ denotes the coefficient at mode k. On each box routed to Lemma 7.4, we bound all corner values of the three numerators and their positive denominator D. These homogeneous quantities are multiaffine in the box coordinates: in an alternating-ear chart, terms quadratic in any single apex cancel identically, so each apex appears at most linearly.

The degrees after substituting $p_i = (1-h_i)s_i$ and in the mixed chart are verified symbolically in `verify_projective_chart.py`. If a homogeneous tuple is $\sum_\nu t_\nu(D_\nu, N_\nu)$ with $t_\nu \ge 0$, $\sum t_\nu = 1$, and $D_\nu > 0$, then its quotient is a convex combination of N_ν/D_ν with weights $t_\nu D_\nu / \sum_\mu t_\mu D_\mu$; thus corner bounds control σ on the entire closed box.

Lemma 7.4. *Let Q be a convex hexagon of the form (7.2). If $0 < \sigma \le 39/200$, then every nonsingular affine image L_1Q satisfies $F(L_1Q) < F(R_6)$. When $\sigma = 0$, $F(L_1Q) \le F(R_6)$ with equality if and only if L_1 is a similarity.*

Proof. Consider first the central ball $0 < \sigma \le 1/20$, where we construct the reference pair by spectral projection of the complex polynomial

$$10^5 p(z) = 205700z - 104432z^2\bar z + 18784z^3\bar z^2 - 2396z^4\bar z^3 + 9491\bar z^5 + 214z\bar z^6 - 2905z^7.$$

Its real and imaginary parts transform like the linear coordinates, are orthogonal, and share the Rayleigh quotient $r_p < 4.044$ by triangle moments. The radial map from $\mathbb{D}$ to R_6 has Jacobian at most 1 and energy distortion below 2 (since $K + K^{-1} \le 7/3$; cf. Proposition 7.7); separation of variables on $\mathbb{D}$ and the Bessel signs in `check_six_local.py` yield $\mu_3(R_6) > 9/2$. Within the rotation types of the linear coordinates, all angular orders other than ±1 have modulus at least 5, and J_1' has only one positive zero below 5, placing the spectrum above the first pair at or above $g_* = 25/2$. The two components of p therefore project injectively into the first cluster, which carries the irreducible planar rotation representation and hence has a single eigenvalue $\lambda = \mu_1(R_6) = \mu_2(R_6)$. Putting $u_i = \Pi_\lambda p_i$ and $\delta_i = p_i - u_i$ in area-averaged norms on R_6, spectral expansion and $\lambda > L$ give

$$\|\delta_i\|_2^2 \le \|p_i\|_2^2 \frac{r_p - L}{g_* - L}, \qquad \|\nabla\delta_i\|_2^2 \le g_*\|p_i\|_2^2 \frac{r_p - L}{g_* - L}.$$

After a physical similarity, the vertices of L_1Q take the form $\omega^j + t\sum_{k=2}^5 d_k\omega^{kj}$ with $t > 0$ and $\sum_{k=2}^5 |d_k|^2 = 1$. On each sector let G send the two radial unit vectors to the corresponding velocities, and write $j_t = \det(I + tG)$ and $a_t = \langle j_t\rangle$ (average over R_6). For a scalar trial f, the exact pulled-back energy minus λ times centered mass is

$$\mathcal{N}(f) = \langle \nabla f^T a_t j_t (I+tG)^{-1}(I+tG)^{-T}\nabla f\rangle - \lambda\big[\langle j_t f^2\rangle - \langle j_t f\rangle^2/a_t\big].$$

On the accepted physical ball, the continuous piecewise-affine fan map is bi-Lipschitz, so $\mathcal{N}(f) < 0$ implies $F(P) < A_0\lambda = F(R_6)$. On (u_1, u_2), the first variation is traceless with smaller eigenvalue $-|B_5|\,|d_5 - \alpha\bar d_3|$, where $|B_5| > 3.579$ and $-0.44 < \alpha = -B_3/B_5 < -0.28$ (from substituting p_i and applying the projection error bounds). Along its kernel, the corrected trials $u_i + th_i$ (archived in `six-polynomials.json`) yield negative quadratic sums in the four dihedral-inequivalent directions:

Velocity	ω^{2j}	$\omega^{3j} + \alpha\omega^{5j}$	ω^{4j}	$i\sqrt{3}\,\omega^{4j}$
Upper bound	-0.48	-2.42	-10.94	-19.87

Across the full ball we keep the mixed term with the residual shear and all higher-order remainders. With $d = \operatorname{tr} G$ and $\epsilon = \det G$, the sector denominator is $1 + td + t^2\epsilon$, and beyond the numerator degree the kinetic coefficients obey $K_k = -dK_{k-1} - \epsilon K_{k-2}$, giving the exact degree-≥ 7 remainder $t^7(K_7 - t\epsilon K_6)/(1 + td + t^2\epsilon)$. Grouping each homogeneous polynomial by its multi-degree (m_j) in the four complex coordinates d_j and writing c_I for its coefficients in $(\operatorname{Re} d_j, \operatorname{Im} d_j/\sqrt{3})$, Cauchy–Schwarz and the binomial theorem bound all phases by

$$\prod_j |d_j|^{m_j} \left(\sum_I \frac{|c_I|^2}{3^{\sum I_j}\prod_j \binom{m_j}{I_j}}\right)^{1/2}.$$

Linear coordinate tests first restrict any affine competitor over $\sigma \le 1/20$ to a shear $z \mapsto z + \tau\bar{z}$ with $|\tau| \le 0.132862$, whence $\|(\xi_2, \xi_3, \xi_4)\| \le (1+|\tau|)\sigma$ and $|\xi_5| = |\tau|$. On each box of normalized amplitudes $|d_k|$, `verify_orbits.py` bounds t and combines the first-order splitting bound with an upper bound on $\sum_i \mathcal{N}(u_i + th_i)/t^2$, yielding 280 negative-trace boxes and 428 infeasible boxes for $t > 0$. Because the weak eigenfunction equation cancels both the zeroth-order terms and the linear terms from the corrections, comparison with the exact λ is needed here.

Next suppose $1/20 < \sigma \le 39/200$. Here we use the fixed pair $p + \eta_0 h$ with rational shear correction $-9\bar{b}/25$, while the affine metric $H = \left(\begin{smallmatrix} e_0 & e_2/2 \\ e_2/2 & e_1/3 \end{smallmatrix}\right)$ ($\det H = 1/3$ in rational coordinates) varies freely. Centering the transported trials yields a 2×2 mass matrix m, and their gradient products define a 3×3 linear stiffness map K. Identifying triples with 2×2 symmetric matrices, a competitor at level $A_0 L$ must satisfy $Z = Ke - Lm \succeq 0$. Set $e_* = K^{-1}Lm$, $Y = H(e) - H(e_*)$, and $s_0 = Z_{11} + 3Z_{22}$. Linear trials and positive semidefiniteness of Z yield

$$0 \le s_0 \le T, \qquad \operatorname{tr}\big(\operatorname{adj} H(e_*)Y\big) \ge w_* s_0, \qquad \det Y \ge -q_* s_0^2.$$

By the two-dimensional determinant identity and concavity of the quadratic lower bound on $[0, T]$, it suffices to check $\det H(e_*) - 1/3 > \max(0, q_* T^2 - w_* T)$. To enclose K^{-1}, we factor out known area terms and normalize K to the identity at the box center; the resulting system $Be = f$ has Taylor coefficients $e_n = f_n - \sum_{j=1}^{n} B_j e_{n-j}$, and an entrywise majorant $D_* \ge |B - I|$ with $\|D_*\|_\infty < 1$ bounds $|B^{-1}| \le (I - D_*)^{-1}$, enclosing the exact truncated residual tail. Solving the transpose equations for rows entering the determinant preserves cancellations. The radial shells, truncation orders N, and correction weights η_0 are given in Table 5.

TABLE 5. Radial shells, Taylor truncation orders N, and correction weights η_0 in Lemma 7.4.

$\sigma_{\min}$	1/20	9/100	11/100	1/8	7/50	9/50
$\sigma_{\max}$	9/100	11/100	1/8	7/50	9/50	39/200
N	8	8	8	8	10	12
η_0	1	1	1	1	4/5	4/5

The scripts `verify_general.py` and `verify_implicit.py` perform exact polynomial operations with outward bounds for square roots and cosines, enclosing all interior phase extrema (detailed conventions and remainder identities appear in `implicit.md`). All six annuli give $F(L_1 Q) < A_0 L < F(R_6)$.

Finally, at $\sigma = 0$, $L_1 Q$ is an affine image of R_6, so Theorem 11.1 (inequality (11.1)) gives $F(L_1 Q) \le F(R_6)$ with equality precisely when the singular-value ratio of L_1 equals 1. □

7.5. **Polynomial Trials Over an Entire Affine Class**

In rational coordinates $\mathbf{X} = (X, Y) = (x, y/\sqrt{3})$ on a normalized polygon P, write $\beta = |P|/A_0$ for its area ratio prior to the free physical affine map. By similarity invariance we may take that affine map to have determinant ± 1, so the constant energy metric E ranges over all 2×2 symmetric positive definite matrices with $\det E = 1/3$. Expectations and covariances below are taken with respect to uniform probability on the normalized polygon. For a rational polynomial pair $f = (f_1, f_2)$, set

$$\Sigma = \frac{\operatorname{Cov}(\mathbf{X})}{\beta}, \qquad M = \frac{\operatorname{Cov}(f)}{\beta}, \qquad (\mathcal{K}E)_{ij} = \mathbb{E}\big[\nabla f_i^T E \nabla f_j\big].$$

Lemma 7.5. *If a physical affine image satisfies $F \geq A_0\ell$, then there exists a symmetric positive definite matrix E with $\det E = 1/3$ such that $E \succeq \ell\Sigma$ and $\mathcal{K}E \succeq \ell M$. In particular, infeasibility of these two constraints with $\det E = 1/3$ excludes the entire affine orbit at level $A_0\ell$.*

Proof. For every constant vector $v \in \mathbb{R}^2$, centering $v\cdot\mathbf{X}$ and $v\cdot f$ gives energies $v^T Ev$, $v^T(\mathcal{K}E)v$ and masses $v^T\operatorname{Cov}(\mathbf{X})v$, $v^T\operatorname{Cov}(f)v$. The Rayleigh principle yields both matrix inequalities, including off-diagonal entries. □

To convert Lemma 7.5 into verifiable scalar inequalities, identify symmetric 2×2 matrices with their $(11, 12, 22)$ entries under the trace pairing $\langle D, E\rangle = \operatorname{tr}(DE)$. Write $c_0 = 1/3$, $G = E - \ell\Sigma \succeq 0$, and $h = \operatorname{adj}\Sigma$. From $\det G \geq 0$ we obtain

$$\langle h, E\rangle \leq \frac{c_0}{\ell} + \ell\det\Sigma, \qquad \operatorname{tr} G \leq \frac{c_0/\ell - \ell\det\Sigma}{\lambda_{\min}(\Sigma)}.$$

For any $W \succeq 0$, put $D_1 = h - \mathcal{K}^*W$ (trace adjoint). Then $E = \ell\Sigma + G$ and $\mathcal{K}E \succeq \ell M$ give the complementary lower bound

$$\langle h, E\rangle \geq \ell\langle W, M\rangle + \ell\langle D_1, \Sigma\rangle + \min\bigl(0, \lambda_{\min}(D_1)\bigr)\operatorname{tr} G.$$

A strict contradiction between these bounds certifies a leaf. A second test solves $\mathcal{K}E_* = \ell M$, writes $E = E_* + \mathcal{K}^{-1}Z$ ($Z \succeq 0$), and applies the determinant inequality of Lemma 7.4. Both tests are implemented in `verify_alternating_triangle.py`, with matrix conventions listed in `affine-metric-test.md` and `implicit.md`.

All required moments are monomial integrals: on the unit barycentric simplex, $s^i t^j$ has average $2i!j!/(i+j+2)!$, giving exact polynomials in the apex coordinates on the base and attached triangles. In the axial chart one may equivalently integrate a polynomial antiderivative along the oriented boundary, cross-checked against simplex integrals in `verify_axial_moments.py`. On a centered parameter box, keeping signed Taylor coefficients through the chosen order and summing absolute values of the remaining coefficients bounds the error. Portable interval arithmetic runs on $2^{-36}\mathbb{Z}$ with outward rounding and overflow guards, while `quadratic_trial.py` and `cubic_trial.py` provide a rational alternative.

7.6. **Geometric Exclusions**

Four geometric tests exclude parameter boxes without calling on polynomial trial pairs. Throughout this subsection we assume a competing physical hexagon P with $F(P) \geq F(R_6) > C$.

An inscribed triangle. Suppose $T \subset P$ has $|T| \geq \frac{4}{5}|P|$. Normalize T to the unit-side equilateral triangle, set $\rho = |P|/|T| - 1$, and let $q|T|$ be the area of $P \setminus T$ projecting orthogonally onto the open sides of T, so $0 \leq q \leq \rho \leq 1/4$. For $k = 4\pi/3$, extend $U = e^{ikx} + 2e^{-ikx/2}\cos(\sqrt{3}ky/2)$ from T to P by nearest-point projection. It has zero mean on T, and on each side ($s \in [0,1]$) its mass and tangential energy densities are $9 - 8\sin^2(\pi s)$ and $4k^2\sin^2(\pi s)$. Each concave exterior strip, normalized to mass 1, is a mixture of triangular tents, so $\mathbb{E}[\sin^2(\pi s)] \leq 1/2 + 2/\pi^2$. Testing both the extended trial and the linear coordinate in the stretched direction (singular-value ratio $S \geq 1$) yields

$$F \leq \frac{4\pi^2}{3\sqrt{3}}\frac{(1+\rho)^2}{1+4\rho-(3-b_0)q}\left(\frac{S+1/S}{2} + c_1 qS\right),$$
$$F \leq \frac{6\sqrt{3}(1+\rho)^3}{S(1+\rho+4q/5)}, \qquad b_0 = \frac{5-16/\pi^2}{3}, \quad c_1 = \frac{2+8/\pi^2}{3}.$$

The second bound comes from a lower bound on each strip's coordinate covariance (reduced in `dominant-triangle.md` to a polynomial on $[0,1]\times[0,1/4]$ whose Bernstein coefficients after one bisection are all at least $43/1200$). If $F \ge C$, the second inequality bounds S from above; substituting into the first with $\rho = x/4$, $q = \rho y$ $(0 \le x, y \le 1)$ gives a polynomial contradiction whose least Bernstein coefficient is $65506945471434840 1/65536000000000000 > 0$ (`check_dominant_triangle.py`).

Two adjacent turns. Any convex polygon with two consecutive exterior turning angles summing to at least $(31/64)2\pi$ satisfies $F < C$. Normalize $|P| = \pi$, choose a conformal disk map balancing $g(r)e^{i\theta}$, and write $Q_0 = f'/f'(0) = 1 + \sum_{k\ge1}\gamma_k z^k$, with

$$g(r) = c_g \sum_{j=0}^{4} \frac{(-33899/40000)^j r^{2j+1}}{j!(j+1)!}, \qquad g(1) = 1.$$

For a competitor with $F \ge C$, (2.2) yields

$$\sum_{k\ge1} \frac{d_k|\gamma_k|^2}{k+1} \le h, \qquad h = \frac{355E}{113C} - M_1, \qquad d_k = M_{\min(k,48)+1} - M_1 - h > 0.$$

Separate a submeasure of mass $31/64$ at the two adjacent prevertices $\xi_\pm = e^{\pm i\phi}$; the normalized residual turning-angle measure is supported on $\operatorname{Re}\xi \le \cos\phi$. Putting $D_r(\xi) = |1 - r\xi_+\bar\xi|\,|1 - r\xi_-\bar\xi|$, the Schwarz–Christoffel formula gives

$$\sqrt{|Q_0(r\xi_+)Q_0(r\xi_-)|} = \exp\!\left(-\int_{\partial\mathbb{D}} \log D_r(\xi)\, d\nu(\xi)\right),$$

where ν is the exterior-turn probability measure. Jensen's inequality bounds this below via the two atoms and upper bounds on the residual logarithmic mean, while the coefficient budget bounds the evaluations above by the norm of the reproducing kernel $\sum(k+1)z^k/d_k$ after subtracting low modes. At the four radii $7/8, 23/24, 79/80, 255/256$, these bounds contradict each other across $(\cos\phi, \operatorname{Re}\gamma_1/2)$ on 1,195 strict and 33 empty boxes (`adjacent-turns.txt`, `check_adjacent_turns.py`). In the mixed `210` chart, $z = \alpha + \eta - 1 \le 0$ means side OC_1 joins parallel supports; for $0 < z \le 1/24$, the exterior triangle off OC_1 has doubled area $1/z$ while $2|P| \le 2 + z$, and the concave-projection variance bound $1/24$ (Lemma 9.3) limits the physical angular deficit from π to $12|P|/(F|T|) \le 12(49/576)/C < \pi/32$. Thus $e \le w/24$ is excluded throughout the mixed chamber.

Corner angles and side ratios. When $F \ge C$, each physical interior angle exceeds $\pi/2 + 2\arctan(1/20)$. Normalize $|P| = 1$; the diameter coordinate and Lemma 9.3 give $\operatorname{diam}(P)^2 \le 24/C$. A unimodular linear map sends the first quadrant to the limiting wedge of cosine $-40/401$ and sine $399/401$, placing the pulled-back polygon inside $[0, 25/16]^2$ as an initial interval along each ray from the corner. For a fixed spline pair U, a unit-trace positive semidefinite weight W, a vector $b \in \mathbb{R}^2$, and a scalar τ, put

$$H = CU^TWU - \sum_{i,j} G_{ij}(\partial_i U)^T W(\partial_j U) + b^TU - \tau,$$

where G is the pullback energy metric. Writing $m = \int_P U$, the Rayleigh inequality gives $\int_P H \le Cm^TWm + b^Tm - \tau$. On the two angular charts (t, vt) and (vt, t), $\int_P H$ is bounded below by integrating $\min_{0\le s\le 25/16}\int_0^s tH\,dt$ over $v \in [0,1]$. Fixed rational certificates refute the resulting inequality on all 76 rectangles of possible values of m (`right-wedge.md`, `check_right_wedge.py`, on a 700×1500 grid with outward interpolation and quadrature errors).

Now let a, b, c be consecutive edge vectors, put $d_1 = \det(a,b)$, $d_2 = \det(b,c)$, and let m_b be twice the maximum area of a triangle in P based on b. If $\det(a,c) > 0$, normalizing b to a unit vertical segment with horizontal span 1 makes the affine invariant $z_b = m_b\det(a,c)/(d_1d_2)$

the slope difference between the adjoining rays (slopes 0 and z_b). For a unimodular physical metric G, the exterior-turn deficit is $\delta = \int_0^{z_b} dt/[(1,t)^T G(1,t)]$. For any concave probability density ρ on $[0,1]$ with maximum m_ρ, the quintic $f(x) = s - \frac{2}{5}s^3 + \frac{1}{25}s^5$ ($s = 2x-1$) satisfies

$$\mathbb{E}_\rho[(f')^2] \le \frac{27}{2}\, m_\rho \operatorname{Var}_\rho(f),$$

certified by the 442 tent-decomposition boxes of `slice_projection.py` (using j-th moments $2(1+t+\cdots+t^j)/[(j+1)(j+2)]$ and multiplying by $t(1-t)$). Testing f on the normalized projection $y - tx$ (support length ≥ 1, unnormalized slice width ≤ 1) gives $\delta \le (27/2)z_b/F$. Since both adjoining interior angles exceed $\pi/2 + 2\arctan(1/20)$, we have $\delta > 4\arctan(1/20)$, forcing $z_b > 4C\arctan(1/20)/(27/2) > 31/200 > 18/125$, above the cutoff used by the frozen axial trees.

The polar second moment. At area A_0, any convex hexagon with $\mu_1 \ge L$ has centroid polar moment divided by A_0 strictly less than $1091/2500$. Choose x_0 balancing $g(r)(x-x_0)/r$ by minimizing $\int_P \int_0^{|x-x_0|} g(t)\,dt\,dx$. With $J = Lg^2 - (g')^2 - g^2/r^2$, the two Rayleigh tests give $\int_P J \le 0$. The positive radial function g in `verify_polar_cap.py` makes $J - (139/200)r^2$ increasing, so by Fejes Tóth's one-site moment theorem for convex hexagons (Gruber [9, Formula (3)]) its integral is bounded below by the integral on the centered equal-area regular hexagon. Since the centroid minimizes the polar second moment and $\langle r^2\rangle_{R_6} = 5/12$, eight rational polynomial intervals certify

$$\frac{4875694526589167354541479409 1}{1117473078201480000000000000000} < \frac{1091}{2500}.$$

7.7. **Joining the Closed Parameter Regions**

Proposition 7.6. *Every strictly convex hexagon of type `111` or `210` is either excluded by a strict spectral or geometric test, or lies in the closed neighborhood of Lemma 7.4.*

Proof. For `111`, order $h_0 \ge h_1 \ge h_2$. Eleven root boxes split h_0 at

$$0,\ \frac{1}{4},\ \frac{3}{10},\ \frac{1}{3},\ \frac{3}{8},\ \frac{5}{12},\ \frac{1}{2},\ \frac{13}{24},\ \frac{7}{12},\ \frac{2}{3},\ \frac{3}{4},\ 1,$$

covering all permitted h_1, h_2 and $s_i \in [0,1]$. The routine `verify_111.py` checks this ordering, the tangential intervals, closed coverage of every parent by its children, maximal-triangle contractions, Lemma 7.5, and the homogeneous tests for Lemma 7.4.

For the `210` bridge, the alternating base UBC_1 has doubled area $D_1 = 1 - u + u(s+t)$. Writing its three intervening vertices V, W, O as $(1-p_i, h_i+p_i, -h_i)$ in cyclic barycentrics and taking determinants in (7.1) gives

$$\begin{aligned} D_1(h_0,h_1,h_2) &= (tr(1-u),\ w\eta,\ u),\\ D_1(p_0,p_1,p_2) &= (r[(1-u)(1-t)+us],\ D_1(1-w) - uw\eta,\ 1-u). \end{aligned}$$

The other alternating base OVW has doubled area $D_0 = v(1-w) + w[v(t+\eta) + us(1-r)]$. Each homogeneous numerator and base determinant is separately affine in (u,r,w) and jointly affine in (s,t,η), verified symbolically in `check_bridge_geometry.py`. Interpolating homogeneous tuples on knot corners and extreme points of the height prism ($s,t \ge 0$, $s+t \le 1$, $0 \le \eta \le 1$, supplemented only with necessary source inequalities) and dividing by the positive base determinant therefore encloses every source image. The remaining charts use the shear of (7.1) directly.

In mixed-ear coordinates, the new alternating base need not maximize area, so p_i can leave $[0,1]$; spectral integration uses the actual barycentrics of the three attached triangles, subject to convexity $(1-p_{i-1})(h_i+p_i) - h_{i-1}h_i \ge 0$ at shared base vertices, source maximality

against OBC_1, and the area-4/5 and angle tests. Two full-height groups cover $0 \le u \le 1/8$ and $1/8 \le u \le 1/4$ (with 89,688 and 92,362 strict polynomial leaves, using only convexity exclusions otherwise), making any later reference to the lower-knot region acyclic. The single root assuming $z \ge 1/24$ is completed by the independent adjacent-turn bound on $z \le 1/24$.

The 31 raw files in `complete-210-manifest.json` are joined in (u, r, w). An independent rational audit (`audit_210_union.py`) collects every coordinate endpoint, enumerates all 168 elementary closed boxes (total volume 1), requires closed containment of each box (including boundary faces) in some raw source box, and checks the v-interval via monotonicity of $u + (1-u)r$. Height fibers over those knots are verified by the individual trees. Recomputed leaf counts appear in Table 6.

TABLE 6. Recomputed leaf counts across the closed hexagon covers.

Leaf classification	`111`	`210` ear	`210` axial
Strict polynomial ($\le A_0 L$)	175,431	369,631	38,868
Fourier neighborhood ($\sigma \le 39/200$)	14,443	991	1
Geometry outside `111`	75	0	0
Convexity exclusions	0	13,441	0
Source or area comparisons	0	27,458	1
Empty contractions	0	131	14
Angle comparisons	0	84	86

Every polynomial leaf uses a threshold at most $A_0 L$, every Fourier leaf certifies $\sigma \le 39/200$, and all split and terminal checks are evaluated on the full closed boxes. □

Proof of Theorem 7.1. A simple polygon with at most six sides that has a reflex or straight angle, or fewer than six sides, has at most five strictly convex vertices; Lemmas 7.3 and 7.2 give $F(P) < 1049/100 < C < F(R_6)$. Every strictly convex hexagon admits one of the three configurations `300`, `111`, or `210`. Configuration `300` has an edge joining parallel supporting lines and is excluded in Section 7.6; configurations `111` and `210` are settled by Proposition 7.6 and Lemma 7.4. Equality can hold only at $\sigma = 0$, i.e., on an affine image of R_6, and Theorem 11.1 forces that image to be similar to R_6 (on R_6 the `111`, `210`, and `300` triangle areas are $3\sqrt{3}/4$, $\sqrt{3}/2$, and $\sqrt{3}/4$, so every affine image of R_6 has only `111` maximizers). Conversely, Euclidean similarities preserve F. □

From the extracted source directory, replay the supporting bounds, both covers, the benchmark, and the local comparison with

```
python anc/verify.py -section hexagon -jobs 4 -workers 2
```

The driver verifies the file hashes and uses arbitrary-precision rational arithmetic for the geometric spectral comparisons.

7.8. **An Eight-Triangle Enclosure for the Regular Hexagon**

Proposition 7.7. *For any regular hexagon R_6 of positive area,*

$$10.50452925 < |R_6|\mu_1(R_6) < 10.50463603.$$

Proof. Give R_6 circumradius 1 with a vertex at $(1, 0)$. We first isolate its first positive eigenspace via the unit disk $\mathbb{D}$. Separation of variables gives $\mu_3(\mathbb{D}) \ge 9$: angular orders $k \ge 3$ have Rayleigh quotient at least $k^2 \ge 9$, while for orders 0 and 2 the root tests on $0 < x \le 3$

are $J_1(x)=0$ and $J_2'(x)=0$. Setting $t=x^2/4\in[0,9/4]$, alternating-series lower bounds for $2J_1(x)/x$ and $4J_2'(x)/x$ are

$$1-\frac{1}{2}t+\frac{1}{12}t^2-\frac{1}{144}t^3,\qquad 1-\frac{2}{3}t+\frac{1}{8}t^2-\frac{1}{90}t^3,$$

which decrease to $223/1024$ and $1/160$. For order 1, the t-derivative of $2J_1'(2\sqrt{t})$ is bounded above by $-3/2+5t/6-7t^2/48+t^3/80$, increasing to $-1131/5120<0$. All three tails alternate with decreasing magnitudes, so order 1 contributes at most one positive root in each of its sine and cosine components up to $x=3$.

The radial map $(r,\theta)\mapsto(rh(\theta),\theta)$ from $\mathbb{D}$ to R_6, with $h(\theta)=\cos(\pi/6)/\cos\delta$ ($|\delta|\le\pi/6$ from the nearest side normal), has Jacobian $h^2\le 1$ and differential $h\left(\begin{smallmatrix}1 & h'/h\\ 0 & 1\end{smallmatrix}\right)$ in orthonormal polar frames. Its energy matrix has smallest eigenvalue at least $1/K$, where $K+K^{-1}=2+\tan^2(\pi/6)=7/3$, giving $1<K<9/5$. By min–max on the full space including constants, $\mu_3(R_6)\ge 9/K>5$. Every nonzero linear coordinate has zero mean and Rayleigh quotient $24/5<5$ (its normalized second moment is $5/24$ by barycentric integration on the six central triangles). Projecting the linear coordinates onto the positive spectral subspace below 5 is therefore injective; by min–max this subspace has dimension 2, and since rotation by $\pi/3$ has no real invariant line, $\mu_1(R_6)=\mu_2(R_6)$ with one odd direction under horizontal reflection.

Impose Dirichlet conditions on the horizontal cut of the upper half-hexagon and Neumann conditions elsewhere; odd reflection gives lowest eigenvalue $\mu_1(R_6)$ and next eigenvalue above $\Lambda=5$. In rational coordinates $(x,y)=(X,\sqrt{3}Y/2)$, the half-hexagon has vertices $(1,0)$, $(1/2,1)$, $(-1/2,1)$, $(-1,0)$. Connecting $(0,1/2)$ to the four vertices and four side midpoints yields eight triangles, on which the witness specifies a continuous degree-8 scalar v vanishing on the cut and a degree-9 vector polynomial $\hat{q}$ on each reference simplex. With cell affine derivative B, $J=\det B>0$, and $H=JB^{-1}\operatorname{diag}(1,4/3)B^{-T}$, the flux obeys $\operatorname{div}\hat{q}=-J\hat{v}$, with canceling normal flux densities across shared edges and zero normal flux on Neumann sides (verified coefficientwise). Omitting the common factor $\sqrt{3}/2$, set

$$m=\sum_K J\int_\Delta \hat{v}^2,\qquad \rho=\frac{1}{m}\sum_K\int_\Delta \nabla\hat{v}^T H\nabla\hat{v},$$
$$\eta^2=\frac{1}{m}\sum_K\int_\Delta (H\nabla\hat{v}-\rho\hat{q})^T H^{-1}(H\nabla\hat{v}-\rho\hat{q}).$$

By the inverse-operator variance bound (3.1) with $\Lambda=5$,

$$\frac{\rho}{1+\Lambda\eta^2/(\rho(\Lambda-\rho))}\le\mu_1(R_6)\le\rho.$$

The standalone checker `check_hex_flux.py` expands the Bernstein arrays to powers, integrates exactly via $\int_\Delta s^i t^j=i!j!/(i+j+2)!$, verifies $0<\rho<5$ and $\eta^2<7864/10^9$, and compares the squared area-scaled endpoints (with $|R_6|^2=27/4$) against the stated decimals. □

Part III. Other Side Counts and Affine Comparison

8. Nonconvex Quadrilaterals and the Square

Theorem 8.1. *Every simple nonconvex quadrilateral P of positive area satisfies*

$$|P|\mu_1(P)<\frac{47}{5}<\pi^2.$$

Combined with the convex theorem of Endo and Osting [3], the square uniquely maximizes the first positive Neumann eigenvalue among all simple quadrilaterals of prescribed area, up to congruence.

Proof. Write $A = |P|$, $F = A\mu_1(P)$, and let Σ be the covariance matrix of the uniform probability measure on P. Linear trial functions give $\mu_1(P)\Sigma \preceq I$; in dimension two, the two eigenvalues of Σ then satisfy

$$\mu_1(P)(\det \Sigma) I \preceq \Sigma.$$

For any nonconstant affine coordinate $X = n \cdot x + h$ and nonconstant polynomial f, centering $f(X)$ yields $\mu_1(P)\operatorname{Var}(f(X)) \le |n|^2 \mathbb{E}[f'(X)^2]$. Using $n^T \Sigma n = \operatorname{Var}(X)$ in the matrix inequality gives

$$F^2 \le \frac{A^2}{\det \Sigma} \frac{\operatorname{Var}(X)\,\mathbb{E}[f'(X)^2]}{\operatorname{Var}(f(X))}, \tag{8.1}$$

where both factors on the right may be evaluated in any affine chart provided X is transported with P.

Label the vertices in boundary order O, B, D, C with D reflex, so the convex hull is $\triangle OBC$. Taking O as origin and interchanging B, C if needed, write

$$D = d\big((1-s)B + sC\big), \qquad 0 < d < 1, \quad 0 < s \le \frac{1}{2}.$$

The quadrilateral is the interior-disjoint union of $\triangle ODB$ and $\triangle ODC$, with area fractions s and $1-s$. Set $t = s/(1-s)$, $U = 1/d$, and $X_0 = (1+t)U$. In the affine coordinates $D = (1,0)$, $C = (0,1)$, we have $B = (X_0, -t)$ and $A = (1+t)/2$. We claim

$$\frac{108 \det \Sigma}{A^2} = 1 + 4s(1-s)\frac{1-d}{d^2}. \tag{8.2}$$

Let Z equal B, C with probabilities $s, 1-s$, independently of (L, M) uniform on $\{L, M \ge 0,\ L + M \le 1\}$; then $LD + MZ$ is uniform on P. With $\bar{Z} = \mathbb{E}Z$ and $v = B - C$, the simplex moments $\mathbb{E}L = \mathbb{E}M = 1/3$, $\mathbb{E}L^2 = \mathbb{E}M^2 = 1/6$, $\mathbb{E}[LM] = 1/12$ give

$$18\Sigma = DD^T + \bar{Z}\bar{Z}^T - \frac{1}{2}\big(D\bar{Z}^T + \bar{Z}D^T\big) + 3s(1-s)vv^T.$$

Using $\det(D, \bar{Z}) = 1 - t$, $\det(D, v) = -(1+t)$, and $\det(\bar{Z}, v) = -X_0$, taking determinants gives $324 \det \Sigma = \frac{3}{4}(1-t)^2 + 3t(1 + U^2 - U)$, which proves (8.2).

Two affine coordinates follow triangular laws on $[0,1]$: $(y+t)/(1+t)$ has mode s because horizontal sections taper linearly from OD to heights $-t$ and 1, while the affine coordinate equal to 0 at O and 1 at B, C takes value d at D on both triangles, so reflecting it about $1/2$ gives mode $1-d$. Pick the coordinate with mode $b = \min(s, 1-d) \in [0, 1/2]$. Since $s(1-s) \ge b(1-b)$ and $(1-d)/d^2 \ge b/(1-b)^2$, (8.2) yields $108 \det \Sigma / A^2 \ge 1 + 4b^2/(1-b)$.

By barycentric integration, the k-th moment of the triangular law with vertex values $0, b, 1$ is $m_k = 2(1 + b + \cdots + b^k)/[(k+1)(k+2)]$. Take $f(x) = -x + 17x^2 - 11x^3$, set $\sigma^2 = m_2 - m_1^2$, $E = \mathbb{E}[(f')^2]$, $V = \operatorname{Var}(f)$, and put

$$P(b) = \left(\frac{47}{5}\right)^2 (1 - b + 4b^2)V - 108(1-b)\sigma^2 E.$$

For $b = u/(2(1+u))$ $(u \ge 0)$, the coefficients of $10080000(1+u)^8 P(b)$ in ascending powers of u are

$$1071552, \quad 79204992, \quad 893284608, \quad 6058543824,$$
$$17555246672, \quad 25492961320, \quad 20271676157, \quad 8549952615, \quad 1502684580.$$

All nine coefficients are positive, including the leading term covering $b = 1/2$, so $P(b) > 0$ on $[0, 1/2]$. Substitution in (8.1) proves $F < 47/5 < \pi^2$ (since $\pi > 31/10$). If straight redundant vertices are permitted, the resulting triangle also satisfies the strict bound, either by [2] or by taking $d = 1$. □

9. A Strict Comparison from the Number of Convex Corners

Theorem 9.1. *Let $n \geq 8$ and let P be a simple polygon with at most $n-1$ strictly convex vertices. If R_n is the regular n-gon of the same positive area A, then*

$$A(\mu_1(R_n) - \mu_1(P)) > \frac{1}{2n^4}. \tag{9.1}$$

In particular, (9.1) holds for every simple nonconvex n-gon, regardless of its number of reflex vertices.

Proof. Rescale to $|P| = \pi$, write $\langle u \rangle = \pi^{-1} \int_{\mathbb{D}} u \, dA$ for the normalized disk average, put $\lambda = \mu_1(\mathbb{D}) = (j'_{1,1})^2$, and set

$$g(r) = \frac{J_1(\sqrt{\lambda}\, r)}{J_1(\sqrt{\lambda})}, \qquad \phi(re^{i\theta}) = g(r)e^{i\theta}, \qquad M_j = 2j \int_0^1 g(r)^2 r^{2j-1}\, dr,$$

with $M = M_1$, $D_0 = 1 - M$, and $B = M_2 - M$. Then g increases from 0 to 1 with $g'(1) = 0$; the Bessel identities $J_0(\sqrt{\lambda}) = J_2(\sqrt{\lambda}) = J_1(\sqrt{\lambda})/\sqrt{\lambda}$ yield $M = 1 - 1/\lambda$, and substituting $r = u^{1/(2j)}$ shows $M_j \uparrow 1$. Put $\kappa = D_0/M = 1/(\lambda - 1)$.

As in Theorem 2.1, choose a Riemann map $f : \mathbb{D} \to P$ with $\langle |f'|^2 \phi \rangle = 0$ and $f'(0) > 0$, and write

$$Q(z) = \frac{f'(z)}{f'(0)} = 1 + \sum_{k \geq 1} \gamma_k z^k, \qquad w_k = \frac{|\gamma_k|^2}{k+1}, \qquad T = \sum_{k \geq 1} w_k, \qquad G = \sum_{k \geq 1} w_k (M_{k+1} - M).$$

The area formula gives $f'(0)^2 = (1 + T)^{-1}$. The real and imaginary parts of ϕ have zero weighted mean, summed disk energy λM, and summed weighted mass $M + G/(1 + T)$, so Rayleigh's principle gives

$$\frac{\lambda}{\mu_1(P)} - 1 \geq \frac{G}{M(1 + T)}. \tag{9.2}$$

Assume P has at most m strictly convex vertices ($m \geq 4$), and set

$$F(s) = \sum_{k \geq 1} |\gamma_k|^2 e^{-ks}, \qquad U(s) = (e^{ms} - 1)^{-1},$$
$$\Phi(s) = (1 - e^{-ms})^{4/m}, \qquad P_m(s) = e^{-ms}(1 - e^{-ms})^{-1-4/m}.$$

Setting $\rho = e^{-s}$ in Lemma 2.2 (with $p \leq m$) converts (2.1) directly into

$$\frac{1}{4} F''(s) + bF'(s) + b^2(1 + F(s)) \geq (1 + b)^2 e^{-ms} \qquad (s > 0,\ b \geq 0).$$

Taking $b = U(s)$ gives $\frac{1}{4} F'' \geq U(1 - F') - U^2 F$, hence $\big(\Phi(1 - F')\big)' \leq 4\Phi U^2 F$. Integrating from s to ∞ (where $\Phi(1 - F') \to 1$) and substituting back yields

$$\frac{1}{4} F''(s) \geq P_m(s) - U(s)^2 F(s) - 4U(s) \int_s^\infty \frac{\Phi(v)}{\Phi(s)} U(v)^2 F(v)\, dv.$$

Multiply by $4W(s)$ for any weight $0 \leq W(s) \leq s^2/2$ and integrate. For $v \geq s > 0$, we have $U(s) \leq 1/(ms)$, $\Phi(v)/\Phi(s) \leq (v/s)^{4/m}$, and $v^2 U(v)^2 \leq e^{-mv}/m^2$. The first error term

contributes at most $2\int_0^\infty v^2U(v)^2F(v)\,dv$, and reversing integration order bounds the second by $\frac{4}{m-2}$ times the same integral. Thus

$$4\int_0^\infty WP_m \le \int_0^\infty WF'' + \ell_m\int_0^\infty e^{-ms}F(s)\,ds, \qquad \ell_m = \frac{2}{m(m-2)}. \tag{9.3}$$

Take the unit measure $d\nu(v) = -d[g(e^{-v/2})^2]$ on $[0,\infty)$, so $\int_0^\infty e^{-jv}\,d\nu(v) = 1 - M_j$. Put $W_0(s) = (s-1+e^{-s})\mathbf{1}_{s\ge 0}$ and

$$W(s) = \frac{1}{D_0}\int_0^\infty e^{-v}(W_0(s) - W_0(s-v))\,d\nu(v).$$

Then $0 \le W \le W_0 \le s^2/2$, and since $\mathcal{L}W_0(x) = [x^2(x+1)]^{-1}$, shifting yields $x^2(x+1)\mathcal{L}W(x) = (M_{x+1}-M)/D_0$ for all $x > 0$. Expanding $P_m(s) = \sum_{j\ge1} c_j e^{-mjs}$ ($c_1 = 1$, $c_{j+1} = c_j(1+4/(mj))$) and applying Tonelli's theorem to (9.3) (all terms are finite because $T < \infty$ and $M_{k+1} \le 1$) gives

$$I_m := 4\sum_{j\ge1} c_j\frac{M_{mj+1} - M}{(mj)^2(mj+1)} \le G + D_0\ell_m T, \qquad G \ge BT.$$

Dividing by $1+T$ and minimizing the maximum of the two lower bounds for G (which intersect at $T = I_m/(B + D_0\ell_m)$), (9.2) yields

$$\frac{\lambda}{\mu_1(P)} - 1 \ge \frac{BI_m}{M(B + D_0\ell_m + I_m)}. \tag{9.4}$$

We now bound $\mu_1(R_n)$ from below. The centered conformal weight of R_n at area π is $w(z) = Z^{-1}|1-z^n|^{-2t}$, where

$$t = \frac{2}{n}, \qquad a_j = \frac{(t)_j}{j!}, \qquad Z = 1 + \sum_{j\ge1}\frac{a_j^2}{jn+1}, \qquad b_h = \sum_{j\ge0} a_{h+j}a_j \quad (h \ge 0),$$

with $(t)_0 = 1$ and $(t)_j = t(t+1)\cdots(t+j-1)$. On real $H^1(\mathbb{D})/\mathbb{R}$ with normalized Dirichlet energy inner product, let T_w be the positive self-adjoint operator with quadratic form $\langle wu^2\rangle - \langle wu\rangle^2$. Because $w \in L^2(\mathbb{D})$ (only corner power singularities) and $H^1(\mathbb{D}) \hookrightarrow L^4(\mathbb{D})$ is compact, T_w is compact with eigenvalues $1/\mu_k(R_n)$ ($k \ge 1$). On $E = \operatorname{span}_{\mathbb{R}}\{\operatorname{Re}\phi, \operatorname{Im}\phi\}$, rotational symmetry makes the compression of T_w scalar:

$$q = \frac{M + \sum_{j\ge1} a_j^2 M_{jn+1}/(jn+1)}{\lambda M Z} \ge \frac{1}{\lambda}. \tag{9.5}$$

The radial map $(r,\theta) \mapsto (r\rho(\theta),\theta)$ from $\mathbb{D}$ to R_n satisfies $|\rho'/\rho| \le h := \tan(\pi/n)$, Jacobian $\rho^2 \le 2\pi/[n\sin(2\pi/n)]$, and pullback Dirichlet matrix of determinant 1 and trace $2 + (\rho'/\rho)^2$. Since $\mu_3(\mathbb{D}) > 9$ (from the degree-3 alternating Bessel truncations as in Proposition 7.7), min–max on the full space including constants gives

$$\mu_3(R_n) > L_3 := 9\,\frac{2 + h^2 - h\sqrt{4+h^2}}{2}\,\frac{\sin(2\pi/n)}{2\pi/n}. \tag{9.6}$$

For $n \ge 8$, $h \le \sqrt{2} - 1 < 5/12$ and $\sin(2\pi/n)/(2\pi/n) > 8/9$, so $q > 1/L_3$. Thus T_w has a two-dimensional top spectral subspace strictly separated from the rest; orthogonal projection from E onto it is injective and intertwines rotations, so its two eigenvalues coincide at $s_1 = 1/\mu_1(R_n)$. Complexifying and taking $e = \phi/\sqrt{\lambda M}$ (unit energy) with $d_e = \|(T_w - q)e\|$, applying the spectral theorem to $(x - s_1)(x - 1/L_3) \ge 0$ gives

$$s_1 \le q + \frac{d_e^2}{q - 1/L_3}. \tag{9.7}$$

To bound d_e, pair $(T_w - q)e$ against unit-energy vectors orthogonal to E. Because $\langle w\phi\rangle = 0$ and ϕ is a disk eigenfunction, the constant mode of Zw drops out, leaving sources (before dividing by $Z\sqrt{\lambda M}$) at signed angular frequencies 1 and $1 \pm hn$ ($h \ge 1$), with radial parts $g(r)\sum_{j\ge1} a_j^2 r^{2jn}$ and $g(r)\sum_{j\ge0} a_{j+h}a_j r^{(2j+h)n}$. Different signed frequencies are energy-orthogonal, so dropping the restriction to $E^\perp$ enlarges d_e^2 into a sum over signed frequencies. At absolute frequency $l \ge 1$, the radial Neumann inverse has positive kernel

$$\frac{1}{2l}\left[\left(\frac{\min(r,s)}{\max(r,s)}\right)^l + (rs)^l\right]$$

against $s\,ds$, so nonnegative sources may be bounded pointwise from above (first replacing g by 1). For powers r^{p-2} and $r^{p'-2}$, their inverse-energy pairing with respect to normalized disk area is

$$K_l(p,p') = \frac{2(p+p'+l)}{l(p+l)(p'+l)(p+p')}, \tag{9.8}$$

obtained by integrating the response $(pr^l/l - r^p)/(p^2-l^2)$ against $2r^{p'-1}\,dr$ (with $p = p'$ by continuity). Choosing nonnegative majorizing sums $\sum_i d_i r^{p_i-2}$ for each radial source and setting $S = \sum_l \sum_{i,j} d_i d_j K_l(p_i,p_j)$ over signed frequencies, (9.5)–(9.7) give

$$\frac{\lambda}{\mu_1(R_n)} - 1 \le \lambda q - 1 + \frac{S}{MZ^2(q-1/L_3)}. \tag{9.9}$$

We treat $n \ge 33$ analytically. Set $K = 4\kappa\zeta(3)$ and $m = n-1$; we prove

$$\frac{\lambda}{\mu_1(P)} - 1 \ge X_m := \frac{K}{m^3}\left(1 - \frac{11}{m^2}\right), \tag{9.10}$$

$$\frac{\lambda}{\mu_1(R_n)} - 1 \le Y_n := \frac{K}{n^3} + \frac{133}{n^5}. \tag{9.11}$$

From $g''(r) = \lambda(-3J_1 + J_3)/(4J_1(\sqrt{\lambda})) \ge -3\lambda/4$ (positivity of J_3 following by integrating $(x^l J_l)' = x^l J_{l-1}$ twice from 0), $g'(1) = 0$, and $0 \le g \le 1$, we get $1 - g(r)^2 \le \frac{3}{4}\lambda(1-r)^2$ and $1 - M_{k+1} \le \frac{3\lambda}{2(2k+3)(2k+4)} \le \frac{3\lambda}{8k^2}$. Writing $H_{j-1} = \sum_{i<j} 1/i$ and $S_s = \sum_{j\ge1} H_{j-1}/j^s$, using $c_j \ge 1 + 4H_{j-1}/m$, $(1+1/(mj))^{-1} \ge 1 - 1/(mj)$, and $4S_3 = \zeta(4)$ (comparing $\zeta(2)^2 = 2\zeta(2,2) + \zeta(4)$ with the shuffle product of iterated integrals $\zeta(2)^2 = 2\zeta(2,2) + 4\zeta(3,1)$, where $\zeta(3,1) = S_3$), we obtain

$$\frac{m^3 I_m}{4} \ge D_0\zeta(3) - \frac{4D_0 S_4 + (3\lambda/8)(\zeta(5) + 4S_5/m)}{m^2}.$$

With $S_4 \le \zeta(3) - \zeta(4) < 1/4$, $S_5 \le \zeta(4) - \zeta(5) < 1/8$, $6/5 < \zeta(3) < 121/100$, $\zeta(5) < 9/8$, $29/100 < D_0 < 3/10$, $\lambda < 17/5$, and $B > 3/20$, we get $I_m \ge I_* := \frac{4D_0\zeta(3)}{m^3}(1 - 6/m^2)$ and $(D_0\ell_m + I_*)/B \le 5/m^2$ for $m \ge 32$. Inserting I_* into (9.4) proves (9.10).

For R_n, $\lambda q - 1 \le \kappa(1 - Z^{-1})$. Setting $x = 1/n$, integrating $(1-z^n)^{-2/n}$ from 0 to 1 gives unnormalized circumradius $\Gamma(1+x)\Gamma(1-2x)/\Gamma(1-x)$, whose square times $\sin(2\pi x)/(2\pi x)$ equals Z. Expanding the convergent logarithmic gamma and sine series cancels all even powers, yielding for $n \ge 32$

$$1 - Z^{-1} \le \log Z = \sum_{\substack{k\ge3\\ k\text{ odd}}} \frac{2(2^k-2)\zeta(k)}{kn^k} \le \frac{4\zeta(3)}{n^3} + \frac{15}{n^5},$$

as the n^{-5} term is $12\zeta(5)$ and the remainder times n^5 is at most $256\zeta(5)/(7n^2(1-4/n^2))$. Also the beta integral for a_{h+j} gives

$$b_h = \frac{1}{\Gamma(t)\Gamma(1-t)}\int_0^1 u^{h+t-1}(1-u)^{-2t}\,du, \qquad \frac{b_{h+1}}{b_h} = \frac{h+t}{h+1-t}.$$

From $a_j \le te^t j^{t-1}$ and $e^{1/8} < 8/7$, $\zeta(15/8) \le 15/7$, we have $b_0 - 1 \le \frac{5}{2}t^2 \le 10/n^2$ and $b_h \le b_1 = b_0 t/(1-t) \le 11/(5n)$ $(h \ge 1)$ for $n \ge 32$. Majorizing by $(b_0-1)r^{2n}$ and $b_h r^{hn}$, (9.8) gives $K_{u\pm1}(u+2,u+2) \le u^{-3}$ $(u \ge 2)$ and $K_1(2n+2,2n+2) < 1/(2n^2)$, whence $S \le 50/n^6 + 2(11/5)^2\zeta(3)/n^5 < 14/n^5$. For $n \ge 32$, $h < 1/10$ and $\sin(2\pi/n)/(2\pi/n) > 99/100$, so $L_3 > 8$ and $[M(1/\lambda - 1/L_3)]^{-1} < 9$. Inserting $Z \ge 1$, $q \ge 1/\lambda$, and $15\kappa + 126 < 133$ into (9.9) proves (9.11).

Since $2 < K < 21/10$, $(n/(n-1))^5 < 6/5$ for $n \ge 33$, and $(1-1/n)^{-3} \ge 1 + 3/n$,

$$n^5(X_{n-1} - Y_n) \ge 3Kn - 11K\left(\frac{n}{n-1}\right)^5 - 133 > 6n - 161 > n.$$

As $X_{n-1}, Y_n < 1$, we obtain $A(\mu_1(R_n) - \mu_1(P)) \ge \pi\lambda(X_{n-1} - Y_n)/[(1+X_{n-1})(1+Y_n)] > 2/n^4$.

Finally, for $8 \le n \le 32$, keep the first $J = 2048$ positive terms of I_{n-1} in (9.4), enclosing $3.3899577166718 < \lambda < 3.3899577166720$ and the moments M_j via alternating Bessel truncations ($i = 11$ lower, $i = 12$ upper) and Machin's formula with outward dyadic rounding to denominator 2^{112}. For $13 \le n \le 32$, (9.9) uses the integral-test tail bounds (from concavity of $s \mapsto s^{1-t}$)

$$\sum_{j>J} a_j^2 \le \frac{a_J^2(J+t)}{1-2t}, \qquad \sum_{j>J} \frac{a_j^2}{jn+1} \le \frac{a_J^2(1+t/J)}{n(2-2t)},$$

keeping three separate source powers for each $0 \le h \le H = 48$ before lumping the tail (and bounding $h > H$ by $b_H^2/(n^3H^2)$). For $8 \le n \le 12$, the regular lower bounds come from full-spectrum Crouzeix–Raviart inertia (`check_regular_fan.py`), while `check_kernel.py` and `check_tail.py` verify all scalar formulas. Table 7 lists the outward-rounded endpoints, completing the proof. □

TABLE 7. Certified endpoints (rounded outward) for $8 \le n \le 32$ in Theorem 9.1.

n	$A\mu_1(P) <$	$A\mu_1(R_n) >$
8	10.594882	10.5951
9	10.611837	10.6121
10	10.622581	10.6228
11	10.629677	10.6299
12	10.634532	10.6348
13	10.637959	10.638154
14	10.640442	10.640758
32	10.649152	10.649195

Small Side Counts and Scalar Verification for $7 \le n \le 12$

Theorem 8.1 treats $n = 4$. For $n = 5$, combine Theorem 2.1 with the regular-fan bound $A\mu_1(R_5) > 10.3500$ from 80 subdivisions per sector. The positive-turn bounds 10.49 and 10.556 cover $n = 6, 7$. Together these extend (9.1) to all $n \ge 4$. For the last two bounds use $q_* = 10.5$ and 10.563 in Lemma 3.1, with 30 subdivisions per sector.

n	4	5	6	7	8–12	13–32	≥ 33
$n^4 A(\mu_1(R_n) - \mu_1(P)) >$	100	6	5	3	89/100	5	2

Here P is a nonconvex quadrilateral when $n = 4$; for every $n \geq 5$, it suffices that P has at most $n - 1$ strictly convex vertices.

An independent scalar calculation replaces the finite-element bounds for $7 \leq n \leq 12$ and raises the scaled gap above $5/n^4$. For $k \geq 1$ and $m \geq 4$, $(k+m)/[(m-1)(2k+3)(2k+4)]$ decreases in both variables and reduces at $k = 1, m = 4$ to $\lambda^2 \leq 12$, so $1 - M_{k+1} \leq D_0(m-1)/(k+m)$ and $(k+1)/(k+m) \leq (M_{k+1} - M)/D_0$. Retaining denominators in (9.3) gives $I_m \leq (1 + \ell_m)G$, and inserting $T \leq G/B$ into (9.2) improves (9.4) to

$$\frac{\lambda}{\mu_1(P)} - 1 \geq \frac{I_m}{M(1 + \ell_m + I_m/B)}.$$

For the lower bound, work in the complex character space where rotation by $2\pi/n$ acts as $e^{2\pi i/n}$. Allowed disk angular frequencies are $1 + jn$ ($j \in \mathbb{Z}$), all of modulus at least $n - 1 \geq 6$ except 1. For order 1, $2J_1'(\sqrt{y}) < 0$ on $[9, 28]$ (its degree-12 Taylor upper bound has all Bernstein coefficients negative on $[9, 28]$), so the second disk eigenvalue in this character exceeds 28 for all $n \geq 7$. Since the radial map commutes with rotation and $L_3 > 15/4 > \lambda$ at $n = 7$, replacing 9 by 28 in L_3 gives a sharper character gap L_{ch}. Projecting the frequency-1 source Riesz representative onto $\mathrm{span}\{\phi\}^\perp$ subtracts $U^2/(\lambda M)$ from S in (9.9), where $U = \sum_{j \geq 1} a_j^2 M_{jn+1}/(jn+1)$. With $J = 3072$, $H = 48$, and six separated source powers, `check_angular_small.py` obtains Table 8.

TABLE 8. Scalar verification for $7 \leq n \leq 12$ in the rotation character space.

n	7	8	9	10	11	12
$A\mu_1(P) \leq$	10.556	10.592392	10.610550	10.621867	10.629256	10.634272
$A\mu_1(R_n) >$	10.559332	10.594869	10.613565	10.624504	10.631385	10.635952

Corollary 9.2. *For every $n \geq 4$ and every simple nonconvex n-gon P,*

$$F(R_n) - F(P) > \frac{5}{n^4}.$$

For $n \geq 5$, the same inequality holds whenever P has at most $n - 1$ strictly convex vertices.

Proof. Multiply each gap by n^4. The main table gives strict lower bounds $100, 6, 5$ for $n = 4, 5, 6$; Table 8 gives strict lower bounds $8, 10, 19, 26, 31, 34$ for $7 \leq n \leq 12$; `check_kernel.py` verifies values strictly above 5 for $13 \leq n \leq 32$; and for $n \geq 33$, (9.10)–(9.11) give $0 < X_{n-1}, Y_n < 1/100$, so $X_{n-1} - Y_n > n^{-4}$ yields $n^4(F(R_n) - F(P)) > \pi\lambda/(1 + 1/100)^2 > 5$. □

Lemma 9.3. *Let X be a unit directional coordinate of uniform area in a positive-area convex polygon P of width w in that direction. Then $\mathrm{Var}(X) \geq w^2/24$, and hence $\mu_1(P) \leq 24/d^2$ for any convex polygon of diameter d.*

Proof. Shift the range of X to $[0, w]$. As in Proposition 6.3, the piecewise-affine concave density of X is a mixture of triangular densities on $[0, w]$ with modes $u \in [0, w]$. Each normalized tent has mean $(w + u)/3$ and variance $(w^2 - wu + u^2)/18 \geq w^2/24$, including the endpoint limits. Since the variance of a mixture is at least the average within-component variance, $\mathrm{Var}(X) \geq w^2/24$. Testing the centered coordinate along a diameter of length d gives $\mu_1(P) \leq 24/d^2$. □

Corollary 9.4. *For every $n \geq 3$, the maximum $M_n = \max_P F(P)$ over simple n-gons is attained, and every maximizer has n strictly convex vertices. For every $n \geq 4$,*

$$M_{n+1} \geq F(R_{n+1}) > M_n + \frac{5}{(n+1)^4}.$$

Proof. For $n = 3, 4$, use [2] and Theorem 8.1 (adding a straight vertex to a triangle keeps $F \leq 4\pi^2/(3\sqrt{3}) < \pi^2$). For $n \geq 5$, normalize $|P| = 1$. By Corollary 9.2 we may take a maximizing sequence of convex n-gons with $F(P_k) \geq F(R_n)/2$, so Lemma 9.3 bounds their diameters by $d^2 \leq 48/F(R_n)$. Translating one vertex to the origin and extracting a convergent subsequence of vertices gives a compact convex hull K of area 1 whose indicators converge almost everywhere. Restricting any smooth ambient function to P_k and subtracting its mean shows $\limsup \mu_1(P_k) \leq \mu_1(K^\circ)$, because restrictions of smooth functions are dense in $H^1(K^\circ)$ on a Lipschitz polygon. If K had fewer than n strictly convex vertices, Corollary 9.2 would give $F(K^\circ) < F(R_n) \leq M_n$, impossible. Thus K° attains M_n with n strictly convex vertices. Applying Corollary 9.2 at $n+1$ to a maximizing n-gon yields the strict inequality. □

10. Affine-Invariant Fourier Coordinates for Convex n-Gons

Index the vertices $p_0, \dots, p_{n-1}$ of a positive-area convex n-gon P counterclockwise. Put $\theta_j = 2\pi j/n$, $e_j = (\cos\theta_j, \sin\theta_j)^T$, $[a, b, c] = \det(b - a, c - a)$, and

$$m_n = \min_{i<j<k} [e_i, e_j, e_k], \qquad \bar{p} = \frac{1}{n}\sum_{j=0}^{n-1} p_j, \qquad A = \frac{2}{n}\sum_{j=0}^{n-1} p_j e_j^T.$$

Lemma 10.1. *The first harmonic matrix A satisfies*

$$\det A = \frac{4}{n^3} \sum_{i<j<k} [p_i, p_j, p_k][e_i, e_j, e_k] \geq \frac{8m_n}{n^3}|P| > 0. \tag{10.1}$$

For the given labeling, the unique representative of the affine class of P with vertex mean zero and first harmonic matrix I is $q_j = A^{-1}(p_j - \bar{p})$, which satisfies $\max_j |q_j| \leq 2n^3/m_n$. Identifying $\mathbb{R}^2$ with $\mathbb{C}$ and putting $\omega = \exp(2\pi i/n)$, its vertices take the form

$$q_j = \omega^j + \sum_{k=2}^{n-2} c_k \omega^{kj}. \tag{10.2}$$

Proof. Let U, V be the $3 \times n$ matrices with columns $(1, p_j^T)^T$ and $(1, e_j^T)^T$. Since $\sum_j e_j = 0$, UV^T has first row $(n, 0, 0)$ and lower-right block $nA/2$. The Cauchy–Binet formula expands $\det(UV^T) = n^3 \det A/4$ into the sum in (10.1). Convexity makes every summand nonnegative, and the fan triangles (p_0, p_j, p_{j+1}) already have doubled areas summing to $2|P|$. Putting $s_d = \sin(\pi d/n)$, a regular triple with cyclic index gaps a, b, c has doubled area $4s_a s_b s_c$; concavity of $\log\sin$ minimizes this on $\{a+b+c = n,\ a, b, c \geq 1\}$ at permutations of $(1, 1, n-2)$, giving $m_n = 4\sin^2(\pi/n)\sin(2\pi/n) > 0$. This proves (10.1), including collinear boundary vertices.

Under $p_j \mapsto Lp_j + b$, the mean becomes $L\bar{p} + b$ and A becomes LA, giving affine invariance and uniqueness of q_j. In terms of the Fourier coefficients x_k of p_j, A is $z \mapsto x_1 z + x_{n-1}\bar{z}$ with $\det A = |x_1|^2 - |x_{n-1}|^2$; thus q has zero constant term and identity first harmonic, giving (10.2). Mapping a maximum-area vertex triangle to $(0, 0), (1, 0), (0, 1)$ bounds all vertex coordinates in $[-1, 1]$ with $|P| \geq 1/2$, whence $\|A\|_{\mathrm{op}} \leq 2\sqrt{2}$ and $\det A \geq 4m_n/n^3$. In dimension two $\|A^{-1}\|_{\mathrm{op}} = \|A\|_{\mathrm{op}}/\det A$, and applying this to $|p_j - \bar{p}| \leq 2\sqrt{2}$ gives $\max_j |q_j| \leq 2n^3/m_n$. □

The $n - 3$ complex coefficients $(c_2, \dots, c_{n-2})$ give $2n - 6$ real shape parameters, with the origin corresponding to the affine class of R_n.

Corollary 10.2. *Send a maximum-area vertex triangle of a convex n-gon affinely onto a centered equilateral triangle T of circumradius 1, and write Q for the image polygon. For every invertible linear map L with singular-value ratio s,*

$$F(LQ) \le \frac{32\sqrt{3}}{s}.$$

In particular, $F(LQ) \ge F(R_n)$ forces $s \le 32\sqrt{3}/F(R_n) < 16\sqrt{3}/5$ for every $n \ge 5$, independently of the triangle type.

Proof. Every barycentric coordinate of every vertex of Q relative to T lies in $[-1, 1]$ by triangle maximality. The three half-planes where each barycentric coordinate is at most 1 meet in $-2T$, so $T \subset Q \subset -2T$. Hence $|Q| \le 3\sqrt{3}$, and the width of Q in every direction is at least the minimal width $3/2$ of T. Taking a unit eigenvector v for $1/s$ in the pullback metric and testing $v \cdot x$, Lemma 9.3 gives $\mathrm{Var}(v \cdot x) \ge 3/32$, so $F(LQ) \le 32\sqrt{3}/s$. The last bound uses $F(R_n) \ge F(R_5) > 10$. □

11. All Affine Images of Regular Polygons

Theorem 11.1. *For every $n \ge 3$ and every invertible real linear map L with singular-value ratio $s = \sigma_{\max}(L)/\sigma_{\min}(L)$,*

$$\frac{F(LR_n)}{F(R_n)} \le \min\left\{\frac{7}{5s},\ \frac{7s + 10/s}{17}\right\}. \tag{11.1}$$

Thus R_n uniquely maximizes F among its affine images, up to similarity.

11.1. Two Spectral Moments and Two Trial Functions

Give R_n circumradius 1 and center 0, and set $c = \cos(2\pi/n)$, $A = |R_n|$. For any unit vector $v \in \mathbb{R}^2$, the zero-mean coordinate $X_v(x) = v \cdot x$ has Rayleigh quotient

$$\mathcal{R} = \frac{A}{\int_{R_n} X_v^2} = \frac{12}{2 + c},$$

since rotation makes the second-moment tensor scalar and barycentric integration gives average $(2 + c)/6$ for $|x|^2$ on a sector triangle.

Suppose $\nu := \mu_3(R_n) > \mathcal{R}$. The two-dimensional linear space gives $\mu_2(R_n) \le \mathcal{R}$, so the spectral subspace E for $(0, \mathcal{R}]$ has dimension 2, and orthogonal projection P_E maps the linear space isomorphically onto E (any vector in the kernel has Rayleigh quotient at least ν). Intertwining with $2\pi/n$-rotations, which act irreducibly on $\mathbb{R}^2$ for $n \ge 3$, forces $\mu := \mu_1(R_n) = \mu_2(R_n)$.

Set $u = P_E X_v$. Expanding X_v in an orthonormal Neumann basis gives $\mathcal{R} \ge p\mu + (1 - p)\nu$ for $p := \|u\|_2^2/\|X_v\|_2^2$, and testing the weak eigenfunction equation with X_v gives $\int_{R_n} \partial_v u = \mu \int_{R_n} X_v u = \mu \|u\|_2^2$. By Cauchy–Schwarz and $\int_{R_n} |\nabla u|^2 = \mu \|u\|_2^2$, the fraction of energy of u in direction v is at least

$$t = \frac{\mu}{\mathcal{R}} \frac{\nu - \mathcal{R}}{\nu - \mu} = x \frac{y - 1}{y - x}, \qquad x = \frac{\mu}{\mathcal{R}}, \quad y = \frac{\nu}{\mathcal{R}}. \tag{11.2}$$

For $x \le 1 < y$ this expression increases in both variables. Below we establish, for all $n \ge 3$,

$$x \ge \frac{5}{7}, \qquad t \ge \frac{10}{17}. \tag{11.3}$$

Let $H = |\det L|\, L^{-1} L^{-T}$ have eigenvalues $1/s, s$, and pick v with $Hv = v/s$. Pulling back X_v gives $F(LR_n)/F(R_n) \le 1/(xs)$, while pulling back u gives $(1 - t)s + t/s$; inserting (11.3)

proves (11.1). Since $(7s+10/s)/17<1$ on $1<s<10/7$ and $7/(5s)<1$ on $s>7/5$ (with $7/5<10/7$), equality forces $s=1$.

11.2. **Analytic Bounds for $n\geq 32$, $n=3$, and $n=4$**

For $n\geq 32$, the radial map $(r,\theta)\mapsto(rh(\theta),\theta)$ from $\mathbb{D}$ onto R_n, with $h=\cos(\pi/n)/\cos\delta$ ($|\delta|\leq\pi/n$), has Jacobian $h^2\leq 1$ and smallest pullback-energy eigenvalue at least $1/K$, where $K+K^{-1}=2+\tan^2(\pi/n)$. By min–max, $\mu_j(R_n)\geq\mu_j(\mathbb{D})/K$. Using $\pi<22/7$, $\sin a\leq a$, and $\cos a\geq 1-a^2/2$ yields $\tan(\pi/n)<1/10$, $K<10/9$, and $\mathcal{R}<81/20$, so $K\mathcal{R}<9/2$.

On $\mathbb{D}$, separation of variables gives $\mu_1(\mathbb{D})>10/3$ and $\mu_3(\mathbb{D})\geq 9$. Indeed, with $z=a^2/4$, the alternating-series lower bounds

$$\begin{aligned}
2J_1'(a) &\geq 1-\frac{3}{2}z+\frac{5}{12}z^2-\frac{7}{144}z^3 && (0\leq z\leq 5/6),\\
\frac{2J_1(a)}{a} &\geq 1-\frac{1}{2}z+\frac{1}{12}z^2-\frac{1}{144}z^3 && (0\leq z\leq 9/4),\\
\frac{4J_2'(a)}{a} &\geq 1-\frac{2}{3}z+\frac{1}{8}z^2-\frac{1}{90}z^3 && (0\leq z\leq 9/4)
\end{aligned}$$

are decreasing and positive at their right endpoints; $(aJ_1')'=(1/a-a)J_1<0$ on $1<a\leq 3$ allows at most one positive root in each order-1 component up to 3, while orders ≥ 3 have Rayleigh quotient at least 9. Thus $x>20/27$, $y\geq 2$, and $t\geq(20/27)/(2-20/27)=10/17$.

For the equilateral triangle of circumradius 1, the explicit Neumann spectrum (for side length 1, the eigenvalues are $16\pi^2(j^2+jk+k^2)/9$, $j,k\geq 0$; see [2]) gives $\mu=16\pi^2/27$ and $\nu=3\mu$, so $x=2\pi^2/27>73/100$ and $t=(3x-1)/2>10/17$. For the square, $\mu=\pi^2/2$ and $\nu=2\mu$, so $x=\pi^2/12>82/100$ and $t=2x-1>10/17$.

11.3. **Exact Finite Comparison for $5\leq n\leq 31$**

For $5\leq n\leq 31$, the standard-library script `verify_affine_regular.py` proves

$$\frac{\mu_1(R_n)}{\mathcal{R}}>\frac{77}{100},\qquad \frac{\mu_3(R_n)}{\mathcal{R}}>\frac{37}{20},$$

which yield (11.3) by monotonicity in (11.2). Divide each central triangle into $q^2=25$ congruent triangles, giving maximum cell diameter $h^2=\max(1,2-2c)/q^2$. In the Crouzeix–Raviart basis $1-2\lambda_i$, each cell has mass matrix $\sin(2\pi/n)I/(6q^2)$ and stiffness matrix $2G/\sin(2\pi/n)$, where G is the three-vertex graph Laplacian with weights $G_{01}^{\mathrm{edge}}=G_{02}^{\mathrm{edge}}=1-c$ and $G_{12}^{\mathrm{edge}}=c$ (index 0 opposite angle $2\pi/n$). At thresholds $a\mathcal{R}$ ($a=4/5,2$), positive scaling gives local shifted blocks $12q^2G-a\mathcal{R}(1-c^2)I$. Enclosing $c\in[c_-,c_+]$ on a 10^{-10} grid via Machin's formula and alternating cosine series, replacing the graph weights by $1-c_+,c_-$ and $(1-c^2)/(2+c)$ by $(1-c_-^2)/(2+c_-)$ yields a lower matrix in the quadratic-form order. Outward-rounded integer-interval Schur elimination produces pivots avoiding zero with negative counts 1 and 3 (including constants) for every $5\leq n\leq 31$, proving $\mu_{1,h}>(4/5)\mathcal{R}$ and $\mu_{3,h}>2\mathcal{R}$. Lemma 3.1 then yields both bounds and finishes the proof of Theorem 11.1.

12. A Corrected Affine Trial and Equal-Area Vertex Triangles

Adding a linear coordinate term to a first eigenfunction sharpens the affine bound of Section 11 and applies to arbitrary planar domains.

Let $\Omega\subset\mathbb{R}^2$ be a bounded connected Lipschitz domain, put $\mu=\mu_1(\Omega)$, $F(\Omega)=|\Omega|\mu$, and $\langle h\rangle=|\Omega|^{-1}\int_\Omega h$. For an invertible linear map L with singular-value ratio $s\geq 1$, the pullback metric $H=|\det L|\,L^{-1}L^{-T}$ has eigenvalues s^{-1},s. Pick a unit vector v with $Hv=s^{-1}v$ and set $X(x)=v\cdot(x-\langle x\rangle)$.

Theorem 12.1. *For any nonzero real first Neumann eigenfunction u of Ω, define*

$$M = \langle u^2 \rangle, \qquad a = \langle \partial_v u \rangle, \qquad \tau = \frac{a^2}{\mu M}, \qquad x_v = \mu \langle X^2 \rangle, \qquad e_v = \frac{\langle (\partial_v u)^2 \rangle}{\mu M}.$$

Then $0 \le \tau \le \min(x_v, e_v)$ and

$$\frac{F(L\Omega)}{F(\Omega)} \le \frac{s - (s - s^{-1})(e_v - \tau)}{1 + 2\tau(s-1) + \tau x_v (s-1)^2} \le \frac{s}{[1 + \tau(s-1)]^2}. \tag{12.1}$$

If every unit direction v admits a first eigenfunction with $\tau \ge 1/2$, then every affine image with $s > 1$ satisfies $F(L\Omega)/F(\Omega) \le 4s/(1+s)^2 < 1$.

Proof. Testing the weak eigenfunction equation with X gives $a = \mu \langle uX \rangle$. Applying Cauchy–Schwarz to (u, X) and to $(\partial_v u, 1)$ gives $\tau \le x_v$ and $\tau \le e_v$. Test the zero-mean function $w = u + (s-1)aX$. Using $H = sI - (s - s^{-1})vv^T$ and $\nabla X = v$, the cross term and coordinate energy from the correction add up to $(s - s^{-1})a^2$, giving

$$\frac{\langle w^2 \rangle}{M} = 1 + 2\tau(s-1) + \tau x_v (s-1)^2 > 0, \qquad \frac{\langle \nabla w^T H \nabla w \rangle}{\mu M} = s - (s - s^{-1})(e_v - \tau).$$

Their quotient gives the first inequality in (12.1), and $e_v \ge \tau$, $x_v \ge \tau$ give the second. For $s > 1$, $(1+s)^2 - 4s = (s-1)^2 > 0$. □

Corollary 12.2. *For every $n \ge 3$ and every affine image of a regular n-gon,*

$$\frac{F(LR_n)}{F(R_n)} \le \min\left\{ \frac{7}{5s}, \frac{289s}{(10s+7)^2} \right\}. \tag{12.2}$$

In particular, $F(LR_n) = F(R_n)$ if and only if $s = 1$ (congruence at fixed area).

Proof. Take $u = P_E X$, where E is the two-dimensional first eigenspace of R_n. Since $\langle uX \rangle = \langle u^2 \rangle$, we have $a = \mu M$. With $p = \langle u^2 \rangle / \langle X^2 \rangle$ and $\mathcal{R} = 1/\langle X^2 \rangle$, (11.3) gives

$$p \ge \frac{\nu - \mathcal{R}}{\nu - \mu} > 0, \qquad \tau = \mu M = \frac{\mu}{\mathcal{R}} p \ge \frac{\mu}{\mathcal{R}} \frac{\nu - \mathcal{R}}{\nu - \mu} \ge \frac{10}{17}$$

in every direction v. Inserting $\tau \ge 10/17$ into (12.1) yields the second bound in (12.2), while testing X directly yields $\mathcal{R}/(s\mu) \le 7/(5s)$. Since $10/17 > 1/2$, every $s > 1$ gives strict inequality. □

Proposition 12.3. *Let Σ be the covariance matrix of uniform area on Ω, and suppose $\mu = \mu_1 = \mu_2 < \nu = \mu_3$. If $2\lambda_{\min}(\Sigma) \ge \mu^{-1} + \nu^{-1}$, then every nonsimilar affine image satisfies $F(L\Omega)/F(\Omega) \le 4s/(1+s)^2 < 1$.*

Proof. For each unit vector v, $\sigma_v := v^T \Sigma v \ge \lambda_{\min}(\Sigma) > 1/\nu$, so $P_E X \ne 0$, and the projection bound with $\mathcal{R} = 1/\sigma_v$ gives $\tau \ge \mu(\nu\sigma_v - 1)/(\nu - \mu) \ge 1/2$. Apply Theorem 12.1. □

Proposition 12.4. *Let $n \ge 5$ be odd, let $v_0, \dots, v_{n-1}$ be distinct points in cyclic order on a nondegenerate ellipse (indices modulo n), and pick $1 \le k \le (n-1)/2$ with $\gcd(k, n) = 1$. If all n triangles (v_i, v_{i+k}, v_{i+2k}) have equal area, then the polygon is affinely regular. In particular, for $n = 7$ this applies when all seven triangles (v_i, v_{i+2}, v_{i+4}) have equal area, and every physical realization satisfies (12.2) with s measured from R_n.*

Proof. Map the ellipse affinely to the unit circle preserving orientation, with image vertices $z_i \in \mathbb{C}$. Since $2k < n$, all triples (z_i, z_{i+k}, z_{i+2k}) have the same orientation. Adjacent equal-area triangles along step k share the chord $z_{i+k}z_{i+2k}$, so $z_i z_{i+3k}$ is parallel to it (the four vertices are distinct because $n \ge 5$ and $\gcd(k, n) = 1$). Using $(b-a)/(\bar{b} - \bar{a}) = -ab$ on the unit circle yields $z_i z_{i+3k} = z_{i+k} z_{i+2k}$, whence $h_i := z_{i+k}/z_i$ obeys $h_{i+2k} = h_i$. Because $\gcd(2k, n) = 1$, all

h_i equal one primitive n-th root of unity h, so the vertices form a rotated regular n-gon in cyclic order. Undoing the affine map and applying Corollary 12.2 completes the proof. □

Corollary 12.5. *Give R_n ($n \geq 3$) circumradius 1 and center 0. Let $T : R_n \to Q$ be the piecewise-affine homeomorphism onto a convex n-gon Q matching successive vertices, fixing 0, and extending affinely on each central triangle, and suppose $\|DT - I\|_{\mathrm{op}} \leq 1/100$ on every triangle. Then every linear map L with singular-value ratio $s \geq 7/5$ satisfies*

$$\frac{F(LQ)}{F(R_n)} \leq \frac{50117513}{50426145} < 1.$$

For $n = 7$, every maximum-area vertex triangle of LQ has $2, 1, 1$ intervening vertices on its three boundary arcs, in some order.

Proof. Set $\delta = 1/100$. The map $S = LTL^{-1} : LR_n \to LQ$ satisfies $\|DS - I\|_{\mathrm{op}} \leq s\delta$ and has local Jacobian between $(1-\delta)^2$ and $(1+\delta)^2$. When $s\delta < 1$, the singular-value ratio of DS (which also bounds the largest eigenvalue of its pullback energy matrix in dimension two) is at most $(1+s\delta)/(1-s\delta)$. Centered mass drops by at most $(1-\delta)^2$ and area grows by at most $(1+\delta)^2$, so Corollary 12.2 gives

$$\frac{F(LQ)}{F(R_n)} \leq \left(\frac{1+\delta}{1-\delta}\right)^2 \frac{1+s\delta}{1-s\delta} \frac{289s}{(10s+7)^2}.$$

The last factor decreases for $s \geq 1$, so on $7/5 \leq s \leq 2$ the right-hand side is at most

$$\left(\frac{101}{99}\right)^2 \frac{51}{49} \cdot \frac{289}{315} = \frac{50117513}{50426145}.$$

For $s \geq 2$, each vertex of R_n moves by at most δ (as $T(0) = 0$) and the inradius of R_n is $\cos(\pi/n) \geq 1/2$, so $Q \supset (1-2\delta)R_n$. Minimizing over constants on this inner polygon gives $\int_Q X_Q^2 \geq (1-2\delta)^4 |R_n|/\mathcal{R}$, and testing X_Q on LQ (using $|Q|/|R_n| \leq (1+\delta)^2$ and $\mathcal{R}/\mu_1(R_n) \leq 7/5$) bounds the ratio by $(7/10)(101/98)^4 = 104060401/131766880$, which is smaller.

For R_7, a vertex triangle with cyclic index gaps (a, b, c) has doubled area $\sin(2\pi a/7) + \sin(2\pi b/7) + \sin(2\pi c/7)$. Gaps $(2, 2, 3)$ give more than $19/10 + 2/7$ (as $\cos(\pi/14) > 19/20$ and $\sin(\pi/7) \geq 2/7$), whereas all other gaps give at most 2 (a gap ≥ 4 contributes a negative sine, and $(1, 3, 3)$ gives less than $1 + 2\pi/7 < 2$), leaving a reference gap above $13/70$. Perturbing each vertex by at most δ changes each doubled determinant by at most $8\delta + 4\delta^2$, and twice this error is $201/1250 < 13/70$. Thus every maximizer in Q, and hence in LQ, has gaps $(2, 2, 3)$, or intervening counts $(2, 1, 1)$. □

13. A Finite Covering Criterion for Fixed Side Count

Proposition 13.1. *Fix $n \geq 5$. Translate the first vertex of a simple n-gon to 0, scale its area to 1, and order its vertices counterclockwise. Let K_n be the closure of the set of strictly convex n-gon configurations with these normalizations and diameter at most 2, and let $U \subset K_n$ be a relatively open semialgebraic neighborhood of all regular configurations in K_n on which strict comparison $F(P) < F(R_n)$ holds for all nonregular configurations. Then the full simple-polygon inequality and uniqueness hold at n if and only if there exist a rational $q < F(R_n)$ and finitely many polynomials $p_1, \ldots, p_k \in \mathbb{Q}[x, y]$ such that for every $P \in K_n \setminus U$, at least one p_j satisfies*

$$\int_P |\nabla p_j|^2 < q \left(\int_P p_j^2 - \left(\int_P p_j \right)^2 \right). \tag{13.1}$$

When U is defined over the real algebraic numbers, verifying (13.1) for proposed witnesses is a sentence over the real closed field of real algebraic numbers.

Proof. By Corollary 9.2 and Proposition 3.3, $F(R_n) \geq F(R_5) > 10$. Lemma 9.3 gives $F(P) \leq 24/d^2 < 10$ for any unit-area convex polygon of diameter $d > 2$, while nonconvex and redundant-vertex polygons are excluded by Corollary 9.2. Thus every possible competitor lies in K_n, which is compact (all vertices lie in the closed disk of radius 2), with every limit point representing a unit-area convex hull on which polynomial integrals depend continuously.

Assume strict global optimality. For each $P \in K_n \setminus U$, choose a rational $q_P \in (F(P), F(R_n))$. Because restrictions of rational polynomials are dense in $H^1(P)$ on a bounded Lipschitz polygon (by Sobolev extension, smoothing, C^1 tensor Bernstein approximation on a bounding rectangle, and rational approximation of coefficients), some $p_P \in \mathbb{Q}[x, y]$ satisfies (13.1) with q_P. By continuity, the strict inequality holds on a relative neighborhood of P; finitely many such neighborhoods cover the compact set $K_n \setminus U$, and taking $q = \max q_P < F(R_n)$ gives the finite witness family. Conversely, centering p_j in (13.1) yields $F(P) < q < F(R_n)$ on $K_n \setminus U$, which combines with the local hypothesis on U.

Fan triangulation from the first vertex writes each integral in (13.1) as a rational polynomial in the vertex coordinates (collapsed triangles contributing zero). Convexity, cyclic order, the shoelace area constraint, and the diameter bound are polynomial, so K_n is semialgebraic, giving the final statement. □

14. How Many Edges Can Lie on a Largest Triangle's Arcs?

As n grows, the number of partitions of intervening vertices among the three boundary arcs of a maximum-area triangle grows quadratically. For large n, conformal-radius stability eliminates all partitions with a short arc. Here an arc includes its two endpoints, so its edge count is one more than its number of intervening vertices.

Theorem 14.1. *Let $n \geq 4096$ and let P be a convex n-gon with $F(P) \geq F(R_n)$. Each of the three boundary arcs of any maximum-area vertex triangle of P contains strictly more than $n/6$ edges.*

Proof. Normalize $|P| = \pi$, and retain from Section 9 the disk notation $\lambda = \mu_1(\mathbb{D})$, $g(r) = J_1(\sqrt{\lambda}\, r)/J_1(\sqrt{\lambda})$, $M = M_1$, $B_0 = M_2 - M$, and $D_0 = 1 - M$. By (9.11) (checked in `check_tail.py`), the regular n-gon satisfies

$$\frac{\lambda}{\mu_1(R_n)} - 1 \leq \frac{4\zeta(3) D_0}{M n^3} + \frac{133}{n^5} \qquad (n \geq 33), \tag{14.1}$$

with $D_0 < 3/10$ and $B_0 > 3/20$. Take the balanced conformal map $f : \mathbb{D} \to P$ with $f(0) = O$ and $f'(z) = \alpha(1 + \sum_{k\geq 1} \gamma_k z^k)$ ($\alpha^2 = (1+T)^{-1} > 0$, $T = \sum_{k\geq 1} |\gamma_k|^2/(k+1)$). As in (9.2), $S := T/(1+T) \leq (M/B_0)(\lambda/\mu_1(P) - 1)$. Using $F(P) \geq F(R_n)$, (14.1), $M < 1$, and $\zeta(3) < 121/100$, we obtain

$$n^3 S < 8 \cdot \frac{121}{100} + \frac{2660}{3n^2}, \qquad T < \frac{10}{n^3} \qquad (n \geq 4096).$$

Set $b = 19999/20000$ and $R_* = 201/200$. We claim $B_b(O) \subset P \subset B_{R_*}(O)$, with strict containment at all vertices. At $t = 1 - 10^{-6}$, Cauchy–Schwarz applied to the primitive of f' yields

$$\max_{|z|=t} |f(z) - O - \alpha z| \leq \alpha\sqrt{T} \left(\sum_{m\geq 2} \frac{t^{2m}}{m} \right)^{1/2} < \alpha\sqrt{14T},$$

since $-\log(1 - t^2) < 14$. Because $\alpha(t - \sqrt{14T}) > b$, Rouché's theorem applied to $f(z) - w$ for $|w - O| \leq b$ gives $B_b(O) \subset P$. If a point of $\overline{P}$ lay at distance $\geq R_*$ from O, convexity would enclose the hull of $B_b(O)$ and that point, whose area exceeds πb^2 by $b^2(x - \arctan x)$

with $x = \sqrt{(R_*/b)^2 - 1} > 1/10$. Using $x - \arctan x = \int_0^x u^2/(1+u^2)\,du$, this excess exceeds $b^2(1/10)^3/[3(1+1/100)] > \pi(1-b^2)$, contradicting $|P| = \pi$.

Let y_1, y_2, y_3 be the three angular gaps of a maximum-area vertex triangle about O, measured as fractions of a full turn. Inscribing an equilateral triangle in $B_b(O)$ bounds the maximum triangle area below by $3\sqrt{3}\,b^2/4$ (triangle area is convex in each vertex separately). If some $y_j \geq 1/2$, its signed area term is nonpositive and the other two sum to at most $R_*^2 < 3\sqrt{3}\,b^2/4$, impossible. Hence all $y_j < 1/2$. If the smallest gap satisfied $y \leq 3/10$, concavity of sin on $[0,\pi]$ would give

$$\frac{3\sqrt{3}\,b^2}{2R_*^2} \leq \sum_{j=1}^{3} \sin(2\pi y_j) \leq \sin(2\pi y) + 2\sin(\pi y) \leq \sin(3\pi/5) + 2\sin(3\pi/10) < \frac{257}{100},$$

whereas the left-hand side exceeds $257/100$. Every arc therefore spans angular fraction $y > 3/10$.

Let p_i be the positive angular fractions of consecutive vertices about O, and let a_i be the area fractions of the fan triangles. By Solynin's conformal-radius fan method [8] (see `sector-stability.tex`), comparing sector capacities and applying the isosceles estimate gives

$$\log \alpha^2 \leq \sum_{i=1}^{n} p_i \log \frac{a_i q(p_i)}{p_i}, \qquad -\log q(p) = \sum_{\substack{k\geq 3 \\ k \text{ odd}}} \frac{2(2^k-2)\zeta(k)}{k} p^k.$$

The relative entropy $\sum_i p_i \log(p_i/a_i)$ is nonnegative and the series has positive coefficients; keeping the first term yields

$$4\zeta(3) \sum_{i=1}^{n} p_i^4 \leq -\log \alpha^2 = \log(1+T). \tag{14.2}$$

If some arc had $m \leq n/6$ edges (put $q = m/n \leq 1/6$), Jensen's inequality on the arc and its complement gives

$$n^3 \sum_{i=1}^{n} p_i^4 \geq \frac{y^4}{q^3} + \frac{(1-y)^4}{(1-q)^3} \geq \frac{(3/10)^4}{(1/6)^3} + \frac{(7/10)^4}{(5/6)^3} > \frac{21}{10},$$

because the middle expression increases in y and decreases in q for $y > q$. On the other hand, (14.2) and $\zeta(3) > 6/5$ yield $n^3 \sum_i p_i^4 < 10/(4\zeta(3)) < 21/10$, a contradiction. □

15. The Remaining Seven-Sided Comparison

For a maximum-area vertex triangle ABC in a strictly convex heptagon, the counts of intervening vertices on the three boundary arcs sum to 4. Up to relabeling and reversal, the four types are $(4,0,0)$, $(3,1,0)$, $(2,2,0)$, and $(2,1,1)$.

Proposition 15.1. *If a convex heptagon P admits a maximum-area vertex triangle of type $(4,0,0)$, $(3,1,0)$, or $(2,2,0)$, then $F(P) < 10.5659 < F(R_7)$.*

Proof. In type $(4,0,0)$, two sides of the maximizing triangle are consecutive polygon edges; the parallel-support argument from Section 7 uses no side count and gives $F(P) < 10.5043$. For $(3,1,0)$ and $(2,2,0)$, scale to $|P| = \pi$ and suppose $F(P) \geq 10.5659$. Balancing a degree-9 radial disk trial at a conformal center O and adding harmonic corrections gives $T < 211621/10^7$, so

$$-\log r(P,O)^2 = \log(1+T) < \frac{21}{1000}.$$

Let p_i be the angular fractions about O, and let δ_i be half the signed difference of the two base angles of the fan triangle on edge i. Keeping skew terms in the fan expansion (14.2) bounds $-\log r(P,O)^2$ below by

$$\sum_{i=1}^{7}\left(\ell(p_i)+\frac{28\zeta(3)}{\pi^2}p_i^2\delta_i^2\right),\qquad \ell(p)=\frac{24}{5}p^4+\sum_{k\in\{5,7,9,11,13\}}\frac{2(2^k-2)}{k}p^{k+1}.$$

The lower bound $\ell(p)+6\ell((1-p)/6)$ puts every p_i strictly in $(1/40,2/9)$. For type $(3,1,0)$ with maximal triangle (V_0,V_4,V_6), replacing V_0 by V_1 forces $\det(V_6-V_4,V_1-V_0)\le 0$; controlling the composite chord direction via adjacent fan angles and base-angle offsets reduces to 1,121 rational four-variable boxes on each of which the fan loss exceeds $21/1000$ (`maximum-310.md`). For type $(2,2,0)$ with maximal triangle (V_0,V_3,V_6), retaining quadratic skew terms from the first six odd powers on both three-edge chains yields 152 terminal boxes (long-chord case) and 11,930 terminal boxes (two-short-chord case), all exceeding $21/1000$ (`maximum-220.md`). Full-spectrum Crouzeix–Raviart inertia on the regular seven-sided fan gives $F(R_7)>10.5659$. □

Proposition 15.2. *Normalize a heptagon P by similarity so that its vertices are $z_j=\omega^j+\sum_{k=2}^{6}\xi_k\omega^{kj}$ ($\omega=e^{2\pi i/7}$). If $0<\rho:=\left(\sum_{k=2}^{6}|\xi_k|^2\right)^{1/2}\le 10^{-8}$, then $F(P)<F(R_7)$. In the notation of Corollary 12.5, if $\delta=\max\|DT-I\|_{\mathrm{op}}\le 4\cdot 10^{-10}$, then every nonsingular affine image LQ satisfies $F(LQ)\le F(R_7)$, with equality precisely when LQ is similar to R_7.*

Proof. Work on the unit-circumradius regular heptagon R_7. Along unit Fourier direction $x=\xi/\rho$, let $K_t=A_t-\mu M_t$ ($\mu=\mu_1(R_7)$) be the area-normalized pulled-back stiffness minus μ times the centered mass, with Taylor coefficients K_j at $t=0$. Let u_1,u_2 be a mass-orthonormal basis of the first eigenspace E. Since $\mu<4<8<\mu_3$, K_0 dominates half the reference energy on $E^\perp$, uniquely defining correctors $h_i\in E^\perp$ by $K_0(h_i,w)=-K_1(u_i,w)$.

For $P_x(t)=\frac12\sum_{i=1}^{2}K_t(u_i+th_i,u_i+th_i)$, the constant and linear terms vanish, and the quadratic form $Q(x)=\frac12\sum_i[K_2(u_i,u_i)-K_0(h_i,h_i)]$ has operator norm at most 5760. On the kernel N of the first-variation matrix, $Q(x)=\frac12\operatorname{tr}D$ for the Schur-reduced matrix $D_{ij}=K_2(u_i,u_j)+K_1(u_i,h_j)$, which is bounded above on N by $-\|x\|^2/8$ by the seven-sided two-mode certificate (`heptagon-local-radius.md`). If $F(P)\ge F(R_7)$, first-order splitting forces $\operatorname{dist}(\xi,N)\le 648\rho^2$. The fan derivative has norm less than 6, and bilinear continuation to $|t|=r:=1/24$ satisfies $|P_x(t)|<180$. Bounding terms of order ≥ 3 by Cauchy's estimate and projecting ξ orthogonally onto N in the quadratic term gives, for $0<\rho\le 10^{-8}$,

$$\frac{P_x(\rho)}{\rho^2}\le-\frac{1-(648\rho)^2}{8}+\rho\left(2\cdot 5760\cdot 648+\frac{180}{r^3(1-\rho/r)}\right)<-\frac{1}{40},$$

contradicting $K_\rho\succeq 0$.

For the affine statement, write $s\ge 1$ for the singular-value ratio of L. The cases $\delta=0$ and $s\ge 7/5$ are covered by Corollaries 12.2 and 12.5. For $1\le s\le 7/5$, Corollary 12.5 bounds $F(LQ)/F(R_7)$ by Ah, where

$$A=\left(\frac{1+\delta}{1-\delta}\right)^2\frac{1+s\delta}{1-s\delta}\le 1+7.1\delta,\qquad h=\frac{289s}{(10s+7)^2},$$
$$1-h=\frac{(s-1)(100s-49)}{(10s+7)^2}\ge\frac{3(s-1)}{17}.$$

If $s-1\ge 42\delta>0$, then $Ah<1$. Otherwise, removing the left orthogonal factor and rescaling leaves a positive matrix with $\|L-I\|_{\mathrm{op}}=\sqrt{s}-1<21\delta$, so each transformed vertex lies within 23δ of its regular counterpart. By Parseval, removing the constant Fourier coefficient and dividing by the first gives $\rho\le 23\delta/(1-23\delta)<10^{-8}$, so the first assertion yields strict comparison unless $\rho=0$, i.e., LQ is regular. □

One can also rule out an explicit open subset of type $(2,1,1)$ away from the regular affine class. In the coordinates of `tied-parameter-exclusion.md`, take $A = B = 1/32$ and allow independent perturbations up to $1/4000$ in each vertex coordinate. Every resulting strictly convex heptagon still has all maximal vertex triangles of type $(2,1,1)$ and contains a parallelogram of area fraction at least $1585433/1722933 > 10/11$; extending two centered cosine trials constantly outside the parallelogram yields $F(LP) < 10.5043$ in every affine position.

Combining Corollary 9.2 (or the circular-mean bound $F(P) < 10.556$ for at most six strictly convex vertices from [7]) with Proposition 15.1, any unresolved seven-sided competitor must be strictly convex with every maximum-area vertex triangle of type $(2,1,1)$. The regular heptagon itself has this type, since strict concavity of $\log\sin x$ on $(0,\pi)$ forces maximal cyclic gaps $2,2,3$. Corollaries 12.2 and 12.5 together with Propositions 12.4 and 15.2 settle affine-regular heptagons, equal-area cyclic configurations on ellipses, an affine neighborhood of R_7, and stretched perturbations. Strict comparison on the full $(2,1,1)$ family, and for arbitrary convex n-gons with $n \geq 7$, remains open.

16. Reproducing the Finite Comparisons

The ancillary files contain the five-sided and six-sided certificates, the verification scripts for Part III, and reference logs. From the extracted source directory, using 64-bit Python 3.11, NumPy, and `python-flint`, run the commands listed in `anc/verification.json`. For example, the hexagonal comparisons are replayed by

```
python anc/verify.py -section hexagon
```

The driver checks the included file digests before running the calculations. The pentagon directory includes a table linking each computation to its proof; the hexagon manifest separates strict spectral leaves, local leaves, and geometric exclusions, and the ancillary driver uses the pure-rational FLINT mode. The Part III scripts replay the nonconvex bounds, the $5 \leq n \leq 31$ spectral ratios of Theorem 11.1, and the heptagon local and angular exclusions. All programs verify finite-dimensional rational or integer-interval inequalities; the passage to Neumann eigenvalue bounds rests solely on the variational and geometric proofs in the text.

Provenance

The pentagonal argument in Part I and the nonconvex hexagonal bound appeared in [7]. Generative AI assisted in developing and checking arguments, implementing the finite comparisons, and preparing both language editions.

References

[1] R. S. Laugesen, Problem 3, in *Low Eigenvalues of Laplace and Schrödinger Operators*, Oberwolfach Report 6/2009, p. 405.

[2] R. S. Laugesen and B. A. Siudeja, Maximizing Neumann fundamental tones of triangles, *J. Math. Phys.* **50** (2009), 112903. doi:10.1063/1.3246834.

[3] R. Endo and B. Osting, Maximizing the fundamental Laplace–Neumann eigenvalue on quadrilaterals, preprint (2026). arXiv:2609.02784.

[4] H. Wang, The Pólya–Szegő inequalities for polygons, preprint (2026), Lemma 3.3. arXiv:2611.22305.

[5] L. E. Payne and H. F. Weinberger, An optimal Poincaré inequality for convex domains, *Arch. Rational Mech. Anal.* **5** (1960), 286–292. doi:10.1007/BF00252910.

[6] L. Dong and H. Wang, Maximizing the first positive Neumann eigenvalue of simple pentagons, Hexagon preprint (2026), hexagon:2611.00671v1.

[7] L. Dong and H. Wang, The first positive Neumann eigenvalue of simple pentagons and the large-side limit, Zenodo, version 1 (18 November 2026). doi:10.5281/zenodo.24356848.

[8] A. Yu. Solynin, Solution of an isoperimetric problem of Pólya–Szegő, *Zap. Nauchn. Sem. LOMI* **168** (1988), 140–153.

[9] P. M. Gruber, A short analytic proof of Fejes Tóth's theorem on sums of moments, *Aequationes Math.* **58** (1999), 291–295.

Soochow University, Suzhou, China

Nanjing University of Information Science and Technology, Nanjing, China